

Determination of thermal and epithermal self-shielding factor using MCNP-Code

Telma Fonseca
CDTN / CNEN

December /2008



Supervisors
P. Vermaercke (SCK.CEN)
E. Malambu (SCK.CEN)
A. Leal (CDTN/CNEN)



Abstract

The irradiation of a sample in the neutron field of a nuclear reactor is affected by the local perturbation of the neutron fluxes produced by the sample. In general, the interpretation of the sample activation due to thermal and epithermal neutrons requires the knowledge of two corrective parameters: the thermal neutron self-shielding factor, G_{th} , and the resonance or epithermal neutron self-shielding factor G_{res} .

Since a year the SCK•CEN – Belgian Nuclear Research Centre - Laboratory of Neutron Activation Analysis (NAA) has undertaken studies to calculate thermal and resonance or epithermal factor self-shielding corrective factors for various dosimeter samples. In the present document, I report the results obtained in that topics during my six month length research training period I have spent at SCK•CEN. Various sample materials used at the K0-NAA laboratory were considered including different foils, filters, liquid samples and powders mixtures.

Key words: NAA, self-shielding G_{th} and G_{ep} factors and MCNP

Resumo

A irradiação de amostras num feixe de nêutrons de um reator nuclear é afetada por uma perturbação local do fluxo de nêutrons produzido pela amostra. Em geral, a interpretação da ativação da amostra produzida por nêutrons térmicos e epitérmicos requer o conhecimento de dois parâmetros de correção: o fator de auto-blindagem para nêutrons térmicos, G_{th} , e o fator de auto-blindagem nêutrons em ressonância ou epitérmico G_{res} .

Desde um ano o SCK•CEN – Centro de pesquisas nuclear da Bélgica – Laboratório de Análises por ativação neutrônica (NAA) iniciou pesquisas para calcular o fator de auto-blindagem para nêutrons térmicos e ressonância ou epitérmicos.

Neste presente trabalho, eu apresento os resultados obtidos neste tópico, durante meus seis meses de pesquisas e treinamento no SCK•CEN. Varias amostras usadas no laboratório K0-NAA foram analisadas levando em conta diferentes folhas, filtros, líquido e misturas em pó.

Key words: NAA, Fator de auto-blindagem G_{th} e G_{ep} e MCNP

Table of contents

1.	Introduction	5
2.	Background and scope of this research	6
2.1.	SCK.CEN and Research activities	6
2.2.	Main research facilities.....	6
2.2.1.	BR3.....	6
2.2.2.	BR2.....	7
2.2.3.	BR1.....	8
2.3.	The ANS institute.....	9
2.3.1.	RMS - Reactor Modelling and Safety	9
2.3.2.	RNM - Reactor and Nuclear Measurements.....	10
2.4.	Neutron Activation Analysis.....	11
3.	Motivation and Objectives of work.....	13
3.1.	Motivation.....	13
3.2.	Objectives of work	13
4.	Theoretical approach.....	14
5.	Samples specification and experimental process.....	17
6.	Monte-Carlo simulation of the sample irradiation process	21
6.1.	MCNP Code	22
6.2.	MCNP modelling.....	23
7.	Results and Discussion.....	26
7.1.	Gold (^{197}Au) foils.....	26
7.2.	Zr foils and ZrO ₂ powders.....	29
7.3.	Chlorine sample.....	32
7.4.	Uranium samples.....	35
8.	Conclusions	37
9.	References	38

Acknowledgments

I would like to thank Dr Peter Vermaercke and Dr Michel Bruggeman for their welcoming me with the RNM expert group. I also Liesel, Leen, Eric, Wim, Eddy, Alex and all people who I spend long time together in the lab for their help and their friendship during my stay.

I would like to thank Dr Edouard Malambu for his wonderful mentoring and his patience during this research work. His permanent availability enables me to remain in contact with him, day and night, receiving almost online (through e-mails) appropriate answers to my numerous questions; to get explanations to my misunderstanding and to learn useful basic knowledge in the field of nuclear radiation physics. His kind attention and his encouraging advises pushed me to give the best of myself and kept me from feeling tired of so a tough research task. This finally made of my six month stay at SCK.CEN an exciting research experience. It enabled me accumulate a valuable background knowledge on reactor dosimetry and Monte-Carlo neutron transport simulations.

I also greatly appreciate the support of Rogério Rivail, of Alexandre Leal of Tuffic Filho and of the faculty and staff members of the Centre of Nuclear Technology Development (CDTN) and Brazilian Nuclear Energy Commission (CNEN) and Institute for Research and Nuclear Energy (IPEN).

I greatly appreciate the help, support and understanding of my family, my special friends Davide D'Alessandro from Italy and Montse Calderer from Spain and also my dear friends who I spend long weekend with in the international SCK Dormitory in Mol-Belgium.

1. Introduction

In the framework of the collaboration between the Brazilian Centre of Nuclear Technology Development (CDTN) and the Brazilian Nuclear Energy Commission (CNEN), I have been involved in the "Instruments and Methods in Physics Research A564" project. From June to December 2008, the opportunity was given me to travel abroad to Belgium for a six month period training and research in the Neutron Activation Analysis laboratory of the Belgian Nuclear Research Centre (SCK•CEN).

During my internship, I worked on the validation of a method to calculate the thermal and epithermal self-shielding factors for dosimeter samples irradiated in neutron fields.

This training program consisted of two phases. The first phase was devoted to the practical training in the laboratory K0-NAA (managed by the RNM expert group) to obtain a background in experimental procedures used to prepare samples, carry out the irradiation and to unfold the measurements. The second phase consisted in a personal research focussed on numerical simulations using the MCNP Monte Carlo transport code to validate the formulas used in the dosimeter analysis to take into account the perturbations induced by thermal and epithermal self-shielding effects. He started by a literature survey on the topic. The simulation phase has been carried out thanks to the helpful support and under the supervision of Dr E. Malambu from the Reactor Modelling and Safety expert group (RMS). The various dosimeter set-ups were modelled for numerical simulations using MCNP5 and/or MCNPX 2.6.F Monte-Carlo code versions running in a parallel computer environment with MPI-multiprocessing.

Various sample materials used at the K0-NAA laboratory were considered including different foils, filters, liquid samples and powders containing various content of nuclides for which the activation is measured.. The experiment I participated in was done with different geometries and irradiation samples containing Cl and Zr. The G-factors were calculated using the formulas developed by Chilian et al [5].

In this report, the main results of this research will be presented. After a short description of the nuclear research environment offered by the SCK•CEN, I will report the outcome of my work focussing on establishing corrective thermal and self-shielding factors for various dosimeter materials and samples investigated.

2. Background and scope of this research

2.1. SCK.CEN and Research activities

The Belgium nuclear program started in the 1950's with the creation of an unconventional non-profit organization called the Research Centre for the Applications of Nuclear Energy (STK-CEAN). STK-CEAN's laboratories found their home in Mol, at one hour's drive north of Brussels, in a superb pinewood of some 200 hectares, bought from the Belgian royal family on December 22, 1953. Construction began shortly thereafter, in 1954. On May 29, 1957, the State authorized the constitution of SCK•CEN as an institute of public utility; it is since then under supervision of the Ministry of Economic Affairs. SCK•CEN is an institution with a legal status according to private law, managed by an independent Board of governors composed of representatives from the industry, the academic world, and the government

Today, SCK•CEN is one of the largest non-academic research centres in Belgium with about 600 employees. The general organization of the centre recently changed and all research activities are now concentrated in three scientific institutes:

- The Institute for Nuclear Materials Science - NMS - develops and assesses new and existing materials for their suitability in nuclear applications;
- The Institute for Advanced Nuclear System - ANS - performs research on the development and the testing of technologies and instrumentation for new reactors;
- The Institute for Environment, Health and Safety - EHS.

Thanks to its know-how, its installations and throughout its more than 50 years of experience, SCK•CEN has earned a reputation as a centre of excellence for research in the nuclear field SCK•CEN provides services to the nuclear industry and the medical sector and is also involved in national and international education and training programmes. Each year, many students can perform their training, Master or PhD thesis research within experimented research teams.

2.2. Main research facilities

SCK•CEN has several research facilities and specialized laboratories for its own research activities and for services to partners and external clients. Only the main facilities will be briefly described hereafter.

2.2.1. BR3

The BR3 (Belgian Reactor 3) was the first PWR (pressurized water reactor) in Western Europe and it is the first to be decommissioned. BR3 was an education centre for the operating personnel of the nuclear power plants expected at that time in Belgium.



Figure 1: BR3 Belgian Reactor PWR

2.2.2. BR2

The BR2 (Belgian Reactor 2) became to operation in January 1963. This Materials Testing Reactor is SCK•CEN's most important nuclear facility. The BR2 indeed has been playing an essential role in the national and international programmes related to:

- the safety of nuclear reactors, plant lifetime evaluations and ageing of components;
- the safety of nuclear fuels, the increase of their burn-up and the use of MOX fuels;
- the evolution and assessment of safety problems;
- production activities related to medical and industrial applications.

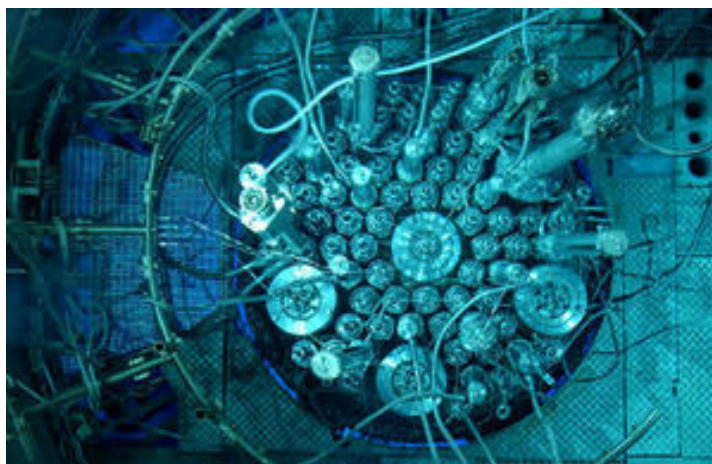


Figure 2: BR2 Belgian Reactor core.

2.2.3. BR1

The BR1 (Belgian Reactor 1) is a 4MWth graphite-moderated and air-cooled reactor. Built in the years 1955-1956, it was the first critical reactor in Europe. Its fuel consists of natural uranium.

Nowadays the reactor is extensively used as a neutron source for neutron activation analysis, dosimetry calibration, neutrography and reference reactor.

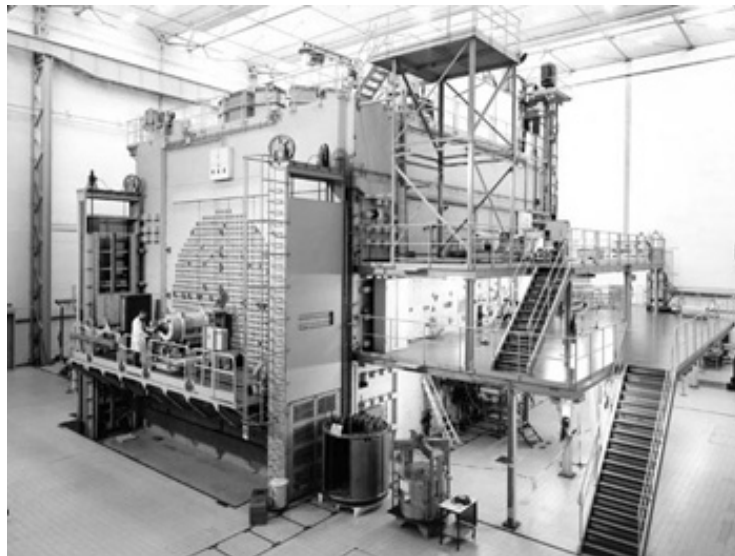


Figure 3: BR1 Belgian Reactor

VENUS



VENUS is a zero-power critical facility that allows the detailed analysis of core configurations, including MOX and high burn-up fuels. It was intensively used for the validation of reactor core configurations and criticality codes. In the framework of the GUINEVERE project, VENUS is being converted into an accelerator-driven system by connected it to the GENEPI deuteron accelerator (developed by CNRS, Grenoble, in France).

This project is carried out in the context of EURATOM FP6 IP-EUROTRANS project and is complementary to MUSE experiments. It aims at validating the subcriticality monitoring for an ADS.

HADES



HADES is an underground laboratory at a depth of 225 m managed by EURIDICE. It allows the study of clay as potential geological host formation for long-lived and highly active nuclear waste.

2.3. The ANS institute

The ANS institute develops and tests technologies and instrumentations for innovative reactors, in collaboration with industry and other international research groups. The research objectives of the ANS institute are multifold depending on the reactor type addressed:

- For research reactors: to develop new experimental devices (with advanced experimentation) for European research reactors such as BR2, Jules Horowitz or the "future" MYRRHA;
- For fusion reactors: to contribute to fusion research and to prepare SCK•CEN to become a partner in the realization of large components for ITER;
- For GEN IV reactors: to take participation in GEN IV activities. Currently, SCK•CEN is active in the design studies of the Lead-cooled Fast Reactor through the European project "ELSY" and follows technologies for SFR and GFR through collaborations with CEA;
- For ADS (Accelerator Driven System): to carry out further development of the MYRRHA/XT-ADS design by completing the conceptual design and conducting the necessary R&D support programme. This R&D support programme covers liquid lead-bismuth technology, advanced instrumentation for MYRRHA and a fuel and material testing and validation programme.

The ANS institute consists of seven expert groups working to fulfil these research goals. My training programme was carried out in synergy between the Reactor and Nuclear Measurements (RNM) and the Reactor Modelling and Safety (RMS) expert groups.

2.3.1. RMS - Reactor Modelling and Safety

This group of engineers and physicists carries out studies in the reactor core physics, shielding and thermal-hydraulics. The ad hoc neutronic team has developed a good expertise in using and even developing neutronics codes both stochastic and deterministic. It is one of the most active MCNPX beta-user group and contribute to the development of the latest MCNPX version through the improvement of the INCL physical model. The group has developed its own MC burn-up code ALEPH which is now used by AREVA (the worldwide leader companies in nuclear reactor building) as a production tool. The JEFF3.1 point-wise energy processed by the group has become one of the official MCNP library available at NEA.

As to the computer platform, the Fermi cluster, depicted in figure 5 and 6 is originated as a set-up of desktop PCs running Linux to support efficiently the neutronics calculations. Over the years, the desktop PCs have been replaced by more powerful servers (first stand-alone, but now in a rack) coupled by Gigabit-Ethernet switches. Currently, about 48 nodes are installed, each having a dual processor layout,

resulting in 96 physical CPUs. Each of these CPUs is a dual core CPU. The memory installed ranges from 1 GB up to 8 GB.



Figure 4: Overview of the cluster



Figure 5: View of Fermi's nodes

2.3.2. RNM - Reactor and Nuclear Measurements

The RNM expert group is specialized in the detection and quantification of neutrons and gamma rays in the following domains, in which it performs research and delivers services:

- Reactor dosimetry
- Reactor physics
- Neutron activation analysis
- Gamma ray spectrometry
- Non-destructive assay
- Preparation of radioactive sources

The laboratory for neutron activation analysis offers an acknowledged "referee method", meaning a primary, accurate and sensitive analytical method for the determination of the concentration of trace elements in solid and liquid samples with Instrumental Neutron Activation Analysis (INAA) using the k_0 -standardisation method.

The k_0 -method is a physical technique based on only nuclear reactions and has the advantage of being quasi absolute, non-destructive, accurate and sensitive with full traceability to SI-units. There is no need for pre-treatment of the sample; INAA obviates the need of complex sample preparation and guarantees the full recovery of the elements to be analysed. The method is generally free of matrix effects and contamination of laboratory chemicals.

- About 69 elements can be determined in concentrations down to the ppb level with an expanded uncertainty of less than 5% (at the 95% confidence level) and a repeatability of less than 1.5% (at 1 sigma level) for samples ranging from about 100 mg to several grams.
- INAA is perfectly suited for routine quality production in a production environment, measurement of trace level contaminants or a complete panoramic elemental characterization of a sample.
- Since INAA is complementary to other techniques, it is very well suited for the validation of these techniques.
- INAA is suitable for the analysis of volatile elements, halogens or "difficult" elements like As and Se where other methods may fail.

2.4. Neutron Activation Analysis

The neutron activation analysis (NAA) is a sensitive non-destructive analytical technique analysis of trace elements. Because the technique is based on nuclear and is matrix independent, INAA can be applied to a wide range of disciplines. The technique itself is already quite old and previously it was mainly used as high-precision research tool for academia, now it is more and more becoming a well-established commercial analysis. The laboratory for neutron activation analysis able to determinate of the concentration of trace elements in solid and liquid samples with Instrumental Neutron Activation Analysis (INAA) using the k_0 -standardisation method. All experimental processes are carried to in the inner irradiation sites (Y4 and S84) of the BR1.

The process of consists in bombarding samples with neutrons and after that measurement of the induced irradiation. The activation process consists in the transmutation of a stable nuclide into radioactive one called radionuclide. Normally the irradiation is done with a flux of neutron in the nuclear reactor and the γ -radiation emitted by the unstable nuclide formed by (n, γ) reaction is measurement. The spectrometry measures gamma rays spectra characteristic of this nuclide. Due the characteristic radiation emitted in the decay – with a specific half-life – of the unstable nuclide formed, is possible to measure qualitative and quantities at concentration of the elements found after at irradiation.

The production rate of a radioactive nuclide is related to the reaction rate by the following equation:

$$dn/dt = NR_s - n\lambda' \quad (1)$$

Solution of equation 1, for the case where R_s and N are constant, yields the following expression for the activity of a foil:

$$A = (\lambda/\lambda') NR_s (1 - (\exp - \lambda' t)) \quad (2)$$

The saturation activity of a foil is defined as the activity when $dn/dt = 0$; thus Eq 2 yields the following relationship for the saturation activity:

$$A_s = (\lambda/\lambda') NR_s \quad (3)$$

The amount of radionuclide produced will depend on the number of target nuclei, the number of neutrons and on the factor called the cross section which defines the probability of activation occurring. If the activation product is radioactive, it will decay with a characteristic half-life, consequently the growth of activity during irradiation will depend on the half-life on the product. The activation of the radionuclide produced (A_0) can be calculation as the equation below:

$$A_0 = N \cdot \Phi \cdot \sigma \cdot (1 - e^{-0,693 t_i/T}) \quad (4)$$

Where

- N is the number of target nuclei,
- Φ is the neutron flux, in neutrons $\text{cm}^{-2} \text{s}^{-1}$,
- σ is the cross section, in barn (10^{-24}cm^2),
- t_i is the irradiation time duration, and
- T , the half-life of the radionuclide product.

Consequently, knowing the activation rate makes it possible to determine the concentration of the element into sample. The number of atoms of the nuclides product, N , is then given by:

$$N = m \cdot C \cdot w \cdot N_0/M^* \quad (5)$$

Where:

C is the concentration of the elements into sample;
 m is the mass of sample, m ,
 w is isotopic abundance of nuclide
 N_0 is Avogadro's number and
 M^* the mass of one mol of atoms of elements.

The energy of the neutrons which are bombarding the nucleus will dictate the type of interaction that occurs and consequently the nature of the activation product. When the nucleus is irradiated in a neutron flux of both slow and fast neutrons, there may be more than one activation product. Similarly, interferences may occur as the result of the same radionuclide being produced by the activation of different target nuclei [13].

3. Motivation and Objectives of work

3.1. Motivation

The irradiation of a sample in the neutron field of a nuclear reactor is affected by the local perturbation of the neutron fluxes by the sample[15]. These variations of neutron flux can be causing interferences in the activation of a target nucleus, so it is necessary an investigated systematically about the problem. This occurs when an element in the sample matrix absorbs neutron in competition with the target of interest. If a material with high cross section to thermal neutrons, would absorb and that reduce the thermal neutrons from the source such that the target would be seeing a lower neutron flux and be activated to a lesser extent that expected. This phenomenon is called of self-shielding and this effect is seen at larger mass of the sample and can be detected by irradiating a set of sample masses and by calculating the induced activity per unit mass. If neutron self-shielding is occurring, then as the mass increases so the activity per unit mass decreases, affecting the concentration of the analysis results. In general, the interpretation of the sample activation due to thermal and epithermal neutrons requires the knowledge of G_{th} and G_{epi} self-shielding factors. This factors can to correct the results found in the analysis process.

In the literature one finds many studies about the calculation in the self-shielding factors. The self-shielding factors can be expressed as a function of parameters depending on the nuclide, on the geometry and on the sample material. In the literature there exist specific formulas expressing G_{th} for various geometries.

3.2. Objectives of work

The objective this work was to validate formulas of resonance self-shielding factors found in the literature and to calculate these factors for various dosimeter materials used at the K0-NAA laboratory. The work achieved included the following tasks:

- the set-up of various irradiation samples models for MCNP simulations;
- The validation of MCNP-code vs. the spreadsheet approach Chilian et al.[5];
- The validation of the MCNP-calculation versus a self-developed program for foils;
- The verification of the results for different filters, liquid samples and powders containing different levels of U and different isotopic ratio's; Experimental part a: dependence of thermal self-shielding on sample geometry and irradiation site using Cl;
- The verification with the MCNP-calculation for G_{th} ; Experimental part b: dependence of epithermal self-shielding on sample geometry and irradiation site using Zr – verification with the MCNP-calculation for G_{ep} ;
- The calculation of the dependence of effecting self-shielding on irradiation site using Zr, Cl and U and verification with the MCNP-calculation for G_{eff} ;

4. Theoretical approach

The K0 standardization method widely used for multi-element neutron analysis program is based in equation that requires the knowledge of thermal and epithermal self-shielding factors, G_{th} and G_{ep} , so the activity A of a given nuclide produced by the (n, γ) reaction upon irradiating a sample containing an amount m of the element is given by

$$A = (mN_{av}\theta/M_{at}) \times \sigma_{th}\phi_{th}(G_{th} + G_{ep}Q_0/f)(1 - e^{-\lambda t_i}) \quad (6)$$

Where:

N_{av} is Avogadro's number,

θ is the isotopic abundance,

M_{at} is the atomic mass,

σ_{th} is the thermal neutron activation cross-section,

$Q_0 = I_0/\sigma_0$, the ratio of resonance integral to 2200 m s⁻¹ cross-section,

$f = \phi_{th}/\phi_{ep}$, ϕ_{th} and ϕ_{ep} , are the unperturbed thermal and epithermal fluxes and

λ the decay constant and t_i is the irradiation time.

In order to separate the activities due to thermal and resonance neutrons, bare and cadmium-covered foils are exposed under identical conditions and the activities measured. The method, called the cadmium-difference method, is based on the fact that cadmium is an effective absorber of neutrons below some energy, E_c , but it passes neutrons of energies above E_c . E_c is known as the “effective cadmium cut-off energy”. Its value depends upon the cadmium thick-shield in an isotropic neutron field, E_c may be taken to be about 0.55eV. The cadmium ratio, R , for a given neutron flux is defined as follows:

$$R = R_B/R_{Cd} \quad (7)$$

Where R_B and R_{Cd} = the reaction rates for the bare and cadmium-covered configurations, respectively. When both resonance and thermal neutrons are present in the radiation field, the expression relating the thermal-fluence rate to the reaction rate, R_s , observed for a bare detector, Eq 12 is modified to read as follows:

$$\Phi_0 = \frac{R_s}{\sigma_0} \frac{R - 1}{R} \quad (8)$$

The knowledge of the thermal-neutron fluence rate is often important in making fast-neutron fluence rate measurements because of interfering activities produced as a result of thermal-neutron absorption by the nuclide being activated, by its activation products, or by impurities in the test specimen. Also there may be a reduction in the measured activity because of the transmutation loss or “burn-up” of the activation product of the fast-neutron reaction due to thermal-neutron absorption. Furthermore, thermal-neutron measurements are necessary in connection with reactor physics analysis and in order to predict the radioactivity in reactor components.

According to Chilian et al. [5] the epithermal or resonance self-shielding factor can be expressed by a universal sigmoid function of the amount m of the element in a cylindrical sample as follows:

$$G_{ep} = \frac{0.94}{1 + (m/m_{ep})^{0.82}} + 0.06. \quad (9)$$

The parameter m_{ep} varies with the radius and height of the cylinder as $r(r+h)$ and can be estimated from the width and position of the resonances, the cross-section at the peak of each resonance, and also includes the mutual self-shielding generated by the isotopes of the given element, other than the isotope that produces the studied (n,γ) reaction. And all this nuclear dependence is expressed by a single nuclear parameter $\sigma_{abs,ep}$, which was called the epithermal neutron absorption cross-section.

$$\frac{1}{m_{ep}} = \frac{N_{av}}{r(r+h)M_{at}} K_{ep} \sigma_{abs,ep}. \quad (10)$$

where K_{ep} is a parameter that depends on the properties of the actual irradiation site, such as the shape of the neutron spectrum and the surrounding reflecting materials.

And the thermal self-shielding factor can be expressed by:

$$G_{th} = \frac{1.00}{1 + (m/m_{th})^{0.964}} \quad (11)$$

Where the m_{th} varies with the radius and height of the cylinder as $r(r+h)$ can be estimated from the thermal neutron absorption cross-section as:

$$\frac{1}{m_{th}} = \frac{K_{th} N_{av} \sigma_{abs}}{r(r+h)M_{at}} (\sigma_{total} / \sigma_{abs})^{0.15} \quad (12)$$

Where the σ_{total} is the element total thermal neutron cross-section (scattering plus absorption) and K_{th} is a parameter which may depend on the irradiation site, but is independent of the nuclide and the sample composition.

According to Martinho et al. [15], most of the materials used in neutron activation analyses (NAA) such as the presence of a sample in an epithermal neutron field originate a flux perturbation due to neutron absorption inside the sample. Consequently, interpretation of the sample activation requires the application of resonance self-shielding factors. The resonance neutron self-shielding factor, G_{res} depends mainly on material properties, reaction cross-section and thickness (for foils) or radius (for wires and spheres). [6]

The resonance self-shielding factor, G_{res} is defined as the ratio between the reaction rates per atom in the real sample and in a similar and infinitely diluted sample. Thus:

$$G_{res} = \frac{\int_{E_1}^{E_2} \phi(E) \sigma_{ny}(E) dE}{\int_{E_1}^{E_2} \phi_0(E) \sigma_{ny}(E) dE} \quad (13)$$

Where $\phi(E) \propto E^{-1}$ is the original, non-perturbed, epithermal neutron flux per unit energy interval inside the infinitely diluted sample, $\phi(E)$ represents the perturbed epithermal neutron flux inside the real sample, $\sigma_{ny}(E)$ designates the (n, γ) cross-section, and E_1 and E_2 are respectively, the lower and upper limits around the energy E_{res} . The total neutron cross-section has been adopted in the calculation of the perturbed neutron flux $\phi(E)$, which takes into account the neutron scattering in the sample. [9]

The reaction rate is related to the fluence rate by the following equation:

$$R_s = \int_0^{\infty} \sigma(E) \Phi(E) dE \quad (14)$$

Where:

$\sigma(E)$ = activation cross section at energy E , and

$\Phi(E)$ = differential neutron fluence rate, that is the fluence per unit energy per unit time for neutrons with energies between E and $E + dE$.

Neutrons with energies extending from those of thermal neutrons to about 0.1 MeV are called resonance neutrons or epithermal neutrons. In this range of energies, the neutron absorption may be divided into two parts. For the first, the cross-section varies as the reciprocal of the neutron velocity. The second is “resonance absorption,” that is characterized by a large increase in cross section over a narrow energy range.

Samples specification and experimental process

For our INAA experiments, we irradiated the samples in the BR1 reactor and afterwards we analyzed them by γ -ray spectrometry. The BR1 irradiation facility is equipped with a rabbit system and on-reactor gamma ray detectors for the analysis of short-lived activation products. The High Purity Germanium (HPGe) detectors are used for analysis of long-lived activation products and the Up-to-date commercial gamma ray spectrum and fitting analysis and k_0 -software.

The BR1 reactor has about 50 channels. Y4 and Y3 channels are parallel to the fuel channels and have a square section of $100 \times 100 \text{ mm}^2$. Channel Y4 presents the highest flux level ($\phi_{\text{th}} = 3.48 \cdot 10^{11} \text{ n/cm}^2\cdot\text{s}$) compared to the other Y channels. Channel Y3 presents a lower flux, but shows a higher fast flux component compared to Y4. The figure 6a shows the irradiation channels penetrations through the BR1 core. Channels Y4 and S84 cross the centre of reactor core. In the figure 6b one sees samples being uploaded in the reactor.

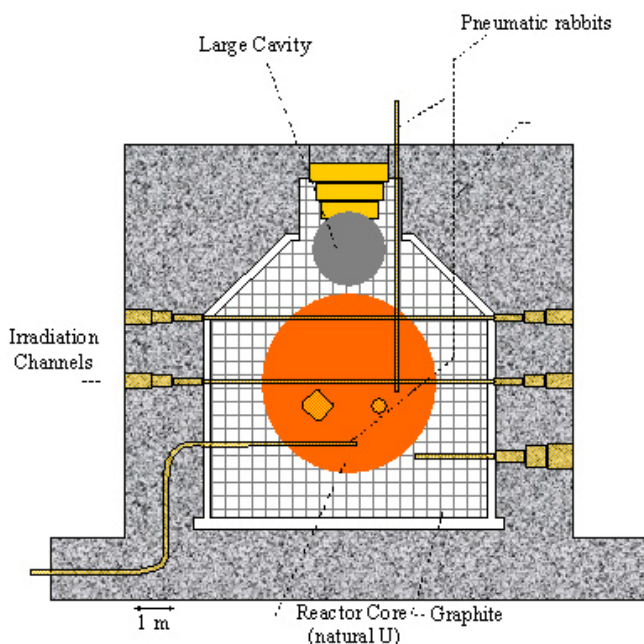


Figure 6: design inner of BR1 Belgian Reactor



Figure 6a: insertion of sample

For the NAA procedure to be successful the specimen or sample must be selected carefully. In many cases small objects can be irradiated and analysed intact without the need of sampling. But more commonly a small sample is taken, usually by drilling in an inconspicuous place. About 50mg (one-twentieth of a gram) is a sufficient sample, so damage to the object is minimised. It is often good practice to remove two samples using two different drill bits made of different materials. This will reveal any contamination of the sample from the drill bit material itself.

The figures 7 and 8 display sets of ZrO_2 and Zr foils samples encapsulated in high purity linear polyethylene vials. The sample vials have various many shapes and sizes to

accommodate many specimen types. These samples were used to determine the G-factors for different heights and different radii.

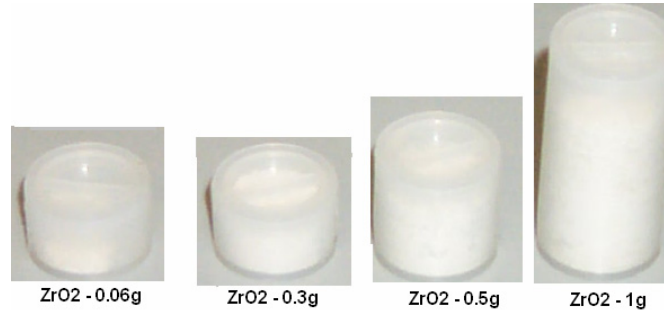


Figure 7: ZrO2 sample used in the experimental process

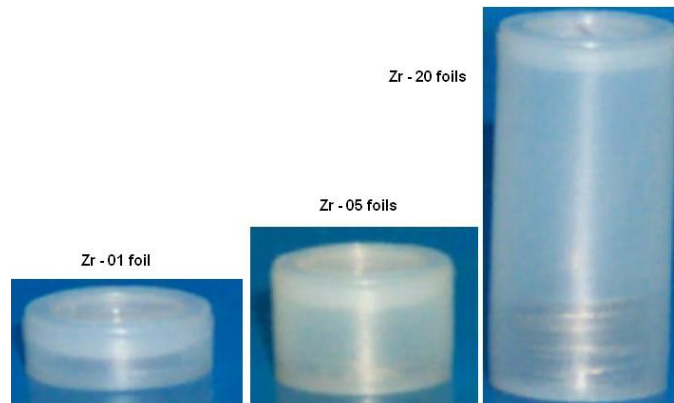


Figure 8: Zr foils sample used in the experimental process

Description	Weight net (mg)	Type Vial	r (mm)	hcorr (mm)	V (mm ³)	d (g/cm ³)
Zr foil 1	32.263	H	3.58	0.127	5.11	6.30935699
Zr foil 5	161.660	V	3.58	0.635	25.55	6.32605769
zr foil 20	680.733	D	3.58	2.54	102.22	6.65958837
ZrO2 0,06	87.137	V	4.05	1.02	52.533927	1.65868049
ZrO2 0,3	409.243	V	4.05	3.23	166.3574355	2.46002229
ZrO2 0,5	683.896	T	4.05	5.5	283.271175	2.41428024
ZrO2 1	1362.782	D	4.05	13.03	671.0951655	2.03068368

Table 1: of the geometries of Zr foils and ZrO2.

Table1 give the specifications of the various Zr foils and ZrO2 powders samples used in the experimental process. The first experimental processes were carried out with 1, 5 and 20 Zirconium foils. In the later cases the foils were stacked inside the vials to obtain different foil height. A to Zr powder, oxide containing 99.8 wt% and 74 WT% respectively were used.

A seven hours long irradiation was carried out in the BR1 Y4-channel in June 2008. For each Zr and ZrO2 sample the activity was measured by counting the γ -rays emitted in the PANORAMIX's germanium detector.. The specific activities were calculated from the areas of the 743Kev from $^{97}\text{Nb-m}$ and 765Kev from ^{95}Zr peaks.

The HyperLab's program was used to analysis all spectra obtained. This program enables to introduce corrections to those spectra when necessary. This process is called deconvolution in which all spectra are put in the database and analyzed.

Afterwards the Kayzero's program was used to calculate the most efficient geometry of samples at different distance and apply corrections such as coincident phenomena.

The same procedure, using the detectors, Hyperlab and Kayzero programs was applied for other samples. To calculate the G_{th} factor self-shielding of Chlorine several samples consisting of a mixture of $C_6H_{12}O_6$ (Sugar) and NH_4Cl . The irradiation of Chlorine mixture samples was carried out in October 2008 inside the S84channel during about 4 hours in the BR1 reactor.

Figure 9 displays the set of NH_4Cl -Sugar samples used in the experimental process to calculate the G-factor of Chlorine



Figure 9: 14 samples of NH_4Cl + Sugar.

The table 2 gives the specifications of the various samples mixtures

Sample	Description	Weight net (mg)	Type Vial	radius	hcorr	V (cm3)	d (g/cm3)	Amount NH_4Cl (g)	Amount Cl (g)	Amount sugar (g)
01	NH_4Cl /sugar 0/100	968.578	R	4.95	12.79	984.0351015	0.98429212	0	0	1
02	NH_4Cl /sugar 8/92	982.36	R	4.95	12.69	976.3413165	1.00616453	0.08	0.05	0.92
03	NH_4Cl /sugar 15/85	987.5305	R	4.95	13.19	1014.810242	0.97311838	0.15	0.1	0.85
04	NH_4Cl /sugar 23/77	967.906	R	4.95	13.19	1014.810242	0.95378028	0.23	0.15	0.77
05	NH_4Cl /sugar 30/70	934.235	R	4.95	13.19	1014.810242	0.92060068	0.3	0.2	0.7
06	NH_4Cl /sugar 38/62	939.3255	R	4.95	13.19	1014.810242	0.92561689	0.38	0.25	0.62
07	NH_4Cl /sugar 45/55	900.5345	R	4.95	13.19	1014.810242	0.88739201	0.45	0.3	0.55
08	NH_4Cl /sugar 53/47	826.778	R	4.95	12.69	976.3413165	0.84681247	0.53	0.35	0.47
09	NH_4Cl /sugar 60/40	798.013	R	4.95	12.69	976.3413165	0.81735044	0.6	0.4	0.4
10	NH_4Cl /sugar 68/32	789.9735	R	4.95	12.69	976.3413165	0.80911612	0.68	0.45	0.32
11	NH_4Cl /sugar 75/25	740.1425	R	4.95	12.69	976.3413165	0.75807762	0.75	0.5	0.25
12	NH_4Cl /sugar 83/17	706.928	R	4.95	12.69	976.3413165	0.72405827	0.83	0.55	0.17
13	NH_4Cl /sugar 91/9	706.6055	R	4.95	12.69	976.3413165	0.72372795	0.91	0.6	0.09
14	NH_4Cl /sugar 98/2	681.9995	R	4.95	13.19	1014.810242	0.67204633	0.98	0.65	0.02

Table 2: of the geometries of Chlorine samples.

Figure 10 show vials containing uranium samples used in the experimental process. These include aqueous U solution,, powders, filter, foils and wire type samples. . The filter sample was made by pouring diluted aqueous solution into the cellulose (paper sheet)



Figure 10: the Uranium samples

Table 3 provide the specifications of the various samples. The main point is the verification of the results for different sample type, namely filters, aqueous solutions and powders containing different amount of U.

To verify variation of the G_{res} as a function of the sample radius, three additional samples vials containing gold (100% Au-197) were prepared.

Type	Sample code	Description	Weight (g)	r (mm)	h (mm)	V (ml)	Side thickness (mm)	D (g/cm ³)
FOIL	81812	Foil with Aluminium=99,8% and Uranium=0.2%	0.03089	6.20	0.10	0.012076	0	2.56
WIRE	81813	Wire with Aluminium=99,8% and Uranium=0.2%	0.02117	2.00	1.00	0.012566	0	1.69
Powder	76705	UO ₂ - Uranium=85,5% Oxide=14,5%	0.01051	4.05	0.03	0.001288	0.65	8.16
FILTER 5.0	81106	Filter spiked with Uranium diluted in water	0.16240	3.85	1.18	0.054948	0.65	2.96
FILTER (Cellulose)	81106	Filter (Cellulose) + U+H ₂ O (100ppm Uranium)	0.03230	3.85	1.37	0.063796		0.51
			0.19470	3.85	2.55	0.118744	0.65	1.64
Liquid	81609	LIQUID with U + H ₂ O (U diluted 100 ppm)	0.13843	4.08	2.55	0.133355	0.65	1.04

Table 3: of the geometries of Uranium samples.

5. Monte-Carlo simulation of the sample irradiation process

Monte Carlo methods are a branch of mathematics that involves the stochastic solution of equations. In a sense, it is (and certainly feels like, when you do it) an experimental approach to solving a problem. When the analyst is trying to use a Monte Carlo approach to estimate a physically measurable variable, the approach breaks itself down into two steps:

1. Devise a numerical experiment whose expected value would correspond to the desired measurable value, \bar{x} .
2. Run the problem to determine an estimate to this variable. We call the estimate \hat{x} .

The first step can either be very simple or very complicated, based on the actual physics of the situation. If the physical situation is itself stochastic, the experimental design step is very simple: Let the mathematical simulation mirror the physical situation. This is called an analog simulation, since the calculation is a perfect analog to the physical situation.

Lucky for us, the physical situation we are looking at - the transport of neutral particles - is a stochastic situation. All we have to do to get a guess at a measurable effect from a transport situation is to simulate exactly the stochastic "decisions" that nature makes in particle transport: the probabilities involved in particle birth, particle travel through material media, particle death, and particle contribution to the desired measurable value (also known as the "effect of interest").

In the basic form of the Monte Carlo method, one carries out a game, or 'experiment' on the computer by simulating the actual physical processes which govern the real particle behavior.

Epithet "MONTE-CARLO" comes from the use of random numbers to determine the outcome of a sequence of chance events.

Unlike deterministic methods of transport modeling (the most common being the discrete ordinates method), which solve the transport equation for average particle behavior, Monte-Carlo methods do not explicitly solve the transport equation. Instead, individual particles are simulated, tracked, and some aspects of their average behavior are scored.

The basic idea of MC is to create a series of life histories of the particles by using random sampling techniques to sample the probability laws that describe the real particle's behavior, and to trace out, step by step, the particle's 'random walk' through the medium. The history of a particle is followed until it can no longer contribute information of interest to the problem at hand. The life history is then terminated and a 'new' particle is started from the source.

A simple example of a problem that can be simulated in this manner is the problem of calculating the number of particles that pass through a slab of absorbing material. In this instance, the primary object in following the life histories of the particles is to count, or 'score', the number of particles that are successful in penetrating the slab. When all particle histories have been simulated, the total score is divided by the total number of

particles simulated, and an estimate obtained for the mean value of the transmitted particles.

Since Monte Carlo is essentially based on statistical concepts, the answer it gives is not unique, rather it is an estimate which should lie within some confidence interval about the ‘true’ answer. Note that the magnitude of the statistical error (uncertainty) associated with the result, the confidence interval, is a function of the number of particle histories simulated. The more histories run, the smaller the confidence interval about the true average behavior of the particles.

The law of large numbers tells us that the accuracy of an estimate of a quantity tends to improve as one averages over larger and larger samples (of independent observations) of the quantity.

Briefly, the (analogue) Monte Carlo process goes as follows: Neutrons are ‘born’/started according to user-specified directives (where in the geometry, direction, energy). Energy and direction are sampled randomly from their cumulative distribution functions. Neutron path lengths between collisions depend on the total macroscopic cross section Σ . The geometry determines whether a neutron leaks out or experiences a collision at the end of its path. Collision types are selected randomly in accordance with the appropriate reaction cross sections. Scattering events change the energy and direction of the neutron before it continues through the system. Leakage, capture or fission terminate the history and signal the start of the next neutron history.

5.1. MCNP Code

MCNP stands for **Monte Carlo for N-Particle Transport**. It is a general purpose code (i.e. not application-specific) for transport of neutrons, photons, and electron transport. Coupled neutron/photon/electron calculations are also possible. That is, induced photons (n, γ) and energetic secondary electrons can also be followed.

The code can calculate eigenvalues (k_{eff} -multiplication factors) for critical systems (kcode-mode) or fixed source calculations (nps-mode). For neutrons, all reactions given in a particular cross-section evaluation are accounted for. Thermal neutrons are described by both the free gas and the $S(\alpha,\beta)$ models (taking into account bounded atoms in some molecules). Extremely accurate modelling of geometry and particle transport is possible. It has the most extensive cross-section tables of any such code. Point-wise rather than ‘multi-group’ cross-section data are used.

To perform any calculation, the user should set-up an input deck file which is read and interpreted by MCNP. This input contains various sections specifying amongst others:

- ✓ the geometry specification of the device to study;
- ✓ the description of materials in the various modelled zones;
- ✓ the choice of cross-section tables to be used;
- ✓ the source characterization and
- ✓ the type of answers desired

A typical complete input file used in for the present study is provided in appendix A .

Monte Carlo methods can calculate directly the self-shielding factor taking into account the dependence on material density and thickness and on atomic mass, natural abundance, and resonance neutron cross-section. This study was done using the MCNP5 the latest MCNP code stable version [1] running in a parallel computer environment with MPI-multiprocessing.

Some back-up calculations have been performed using the MCNPX 2.6.0 code [*] much more indicated in case of fixed source problem in neutron multiplying media, as is the case for uranium samples.

MCNPX 2.6.0 is the latest general-distribution MCNPX version available from RSICC and OECD/NEA. MCNPX (MCNP eXtended) is a general purpose Monte Carlo radiation transport code that tracks nearly all particles at nearly all energies. The official release date of MCNPX 2.6.0 is April 30, 2008. MCNPX began in 1994 as a code-merger project of MCNP 4B and LAHET 2.8. It was first released to the public in 1999 as version 2.1.5. Many new tally source and variance-reduction options have been developed. MCNPX is released with libraries for neutrons, photons, electrons, protons and photonuclear interactions. The 'mesh' and 'radiography' tallies were included for 2 and 3-dimensional imaging purposes.

As to the nuclear data library, the continuous energy cross-section from JEFF-3.1 have been used.

5.2. MCNP modelling

The simulation with MCNP code was prepared take into account all features the sample such as geometry, physical and nuclear properties of the material as well as on the typical dimension of the sample.

The adopted MCNP model considers an isolated sample, as depicted in Figure 11 below, in the isotropic neutron field from the BR1 core. The incoming neutrons from the BR1 core were modelled as point isotropic source sampled on imaginary spherical shell enclosing the sample vial.

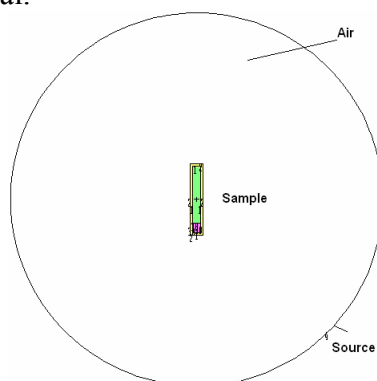
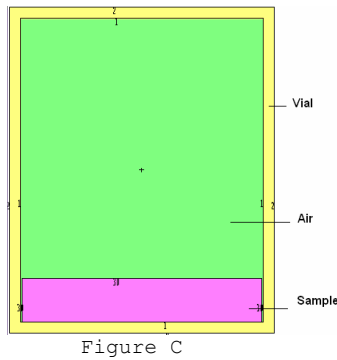
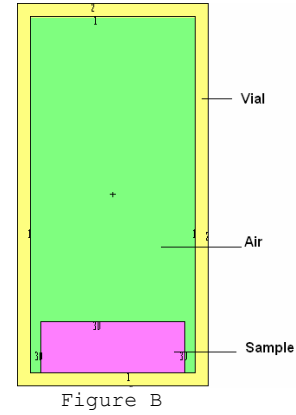
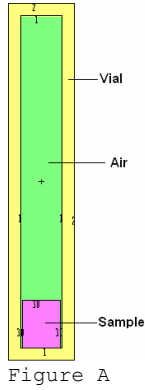


Figure 11: typical geometrical model of the irradiated sample.

The centre of active sample component is taken as the centre of the spherical shell. Figures A, B and C display zoom-views of polyethylene vials of various sizes: with height=18.97mm and radius = 1.00 mm (in figure A), 3.58 mm (in figure B) and 7.00 mm (in figure C). The useful height of sample inside in the vial of polyethylene is 2.54 mm corresponding to the thickness of 20 stacked gold foils ..



The spectrum of source used is showed in Figure 12.. The energy distributions specifying the incoming neutron spectrum was obtained from prevoius full core MCNP modelling of the BR1 reactor.

A reactor neutron spectrum can be considered as being divided into three idealized energy ranges describing the neutrons as thermal, resonance or epithermal, and fast. Since these ranges have distinctive distributions, they are a natural division of neutrons by energy for thermal reactor spectra.

In Figure 12 the neutron spectrum has been plotted both in lethargy unit, $S(U)$ and in energy unit, $S(E)$. The lethargy, U , is defined as:

$$U = \ln(E_0/E) \quad (22)$$

where E_0 is an arbitrarily chosen upper energy limit; The relationship between $\Phi(U)$ and $\Phi(E)$ is:

$$\Phi(U) = \Phi(E)E \quad (23)$$

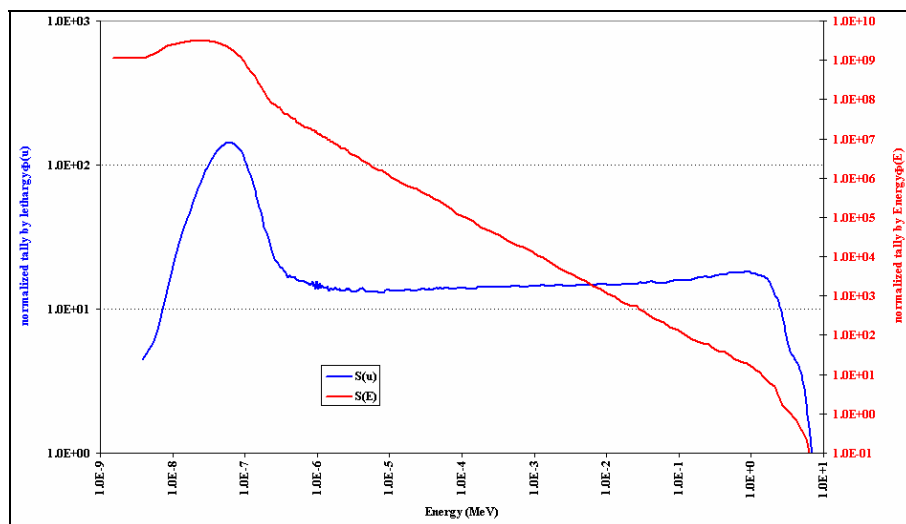


Figure 12: Neutron spectrum (in lethargy and energy units) inside BR1 irradiation channel

6. Results and Discussion

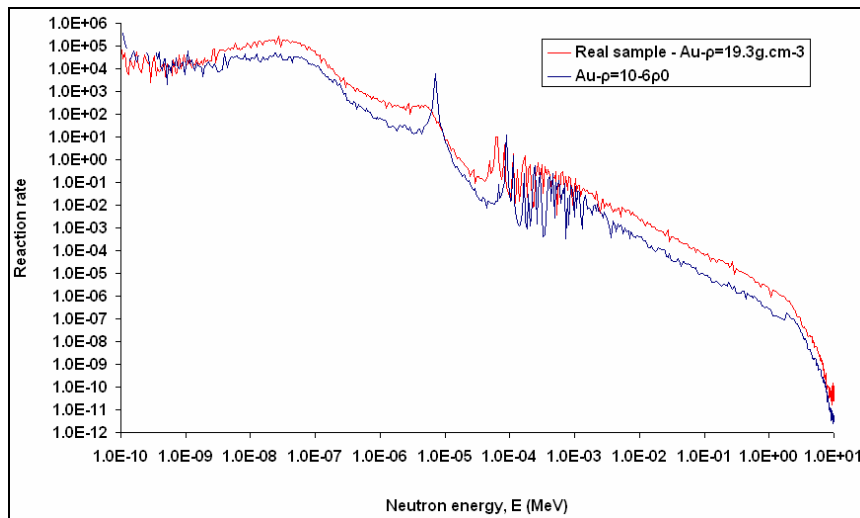
The resonance self-shielding factor, G_{res} is defined as the ratio between the reaction rates per atom in the real sample and in a similar and infinitely diluted sample. In the first moment was studied the density that should be used to dilute the sample. After the simulation with the results, the measurements of reaction rate for each, diluted and “real” sample is possible to calculate the G_{res} factor, but is necessary to compare both reaction rate taking in account the number of atoms in the material.

The epithermal self-shielding factor G_{ep} and M_{ep} factor of Zr and ZrO₂ were calculated according to equation 21 and 22 respectively from Chilian et al. [5]

In order to define the density corresponding to “infinite dilution” for the calculation of the non-perturbed reaction rate, the dependence of the reaction rate on the density was first studied. An input file was developed to calculate the reaction rate of Au-197. To validate the methodology the results are compared with available values obtained by the other authors, such as Gonçalves et al. [8].

6.1. Gold (¹⁹⁷Au) foils

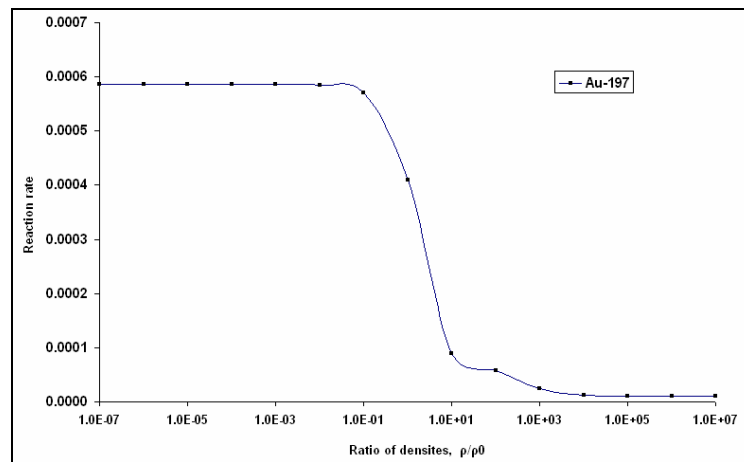
Series of simulations were carried out varying the material density number. In Figure 13 the Au-197 (n,γ) reaction rate is displayed as a function of neutron energy both for to “real” density ($\rho_0 = 19.3 \text{ g.cm}^{-3}$) and for the imaginary “infinite dilution” case ($\rho = 10^{-6} \rho_0 \text{ g.cm}^{-3}$). One observes a well-defined resonance peak at $E_{res} = 4.91 \text{ eV}$.



Graphic 2: Reaction rate versus the neutron energy (MeV) in the “real” density and diluted sample.

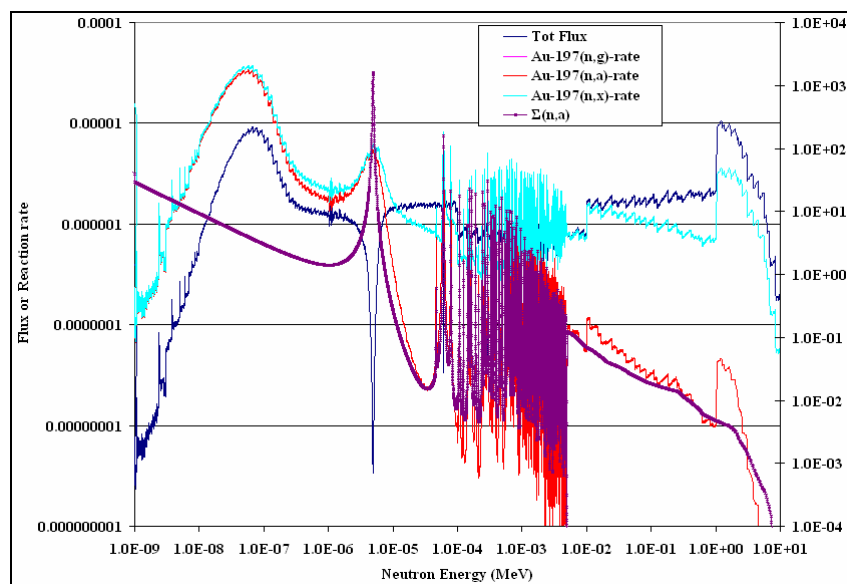
In graphic 3 the variation of the reaction rate per atom of gold is shown as a function of the sample density ratio (ρ/ρ_0). The reaction rate increases as the density ratio decreases and it saturates for $\rho/\rho_0 < 10^{-2}$. For this reason, in all calculations the density for infinite dilution was assumed to be $\rho = 10^{-6}$.

Very similar curve profile can be found in the ad-hoc literature, namely in the paper published by Gonçalves et al. [8].

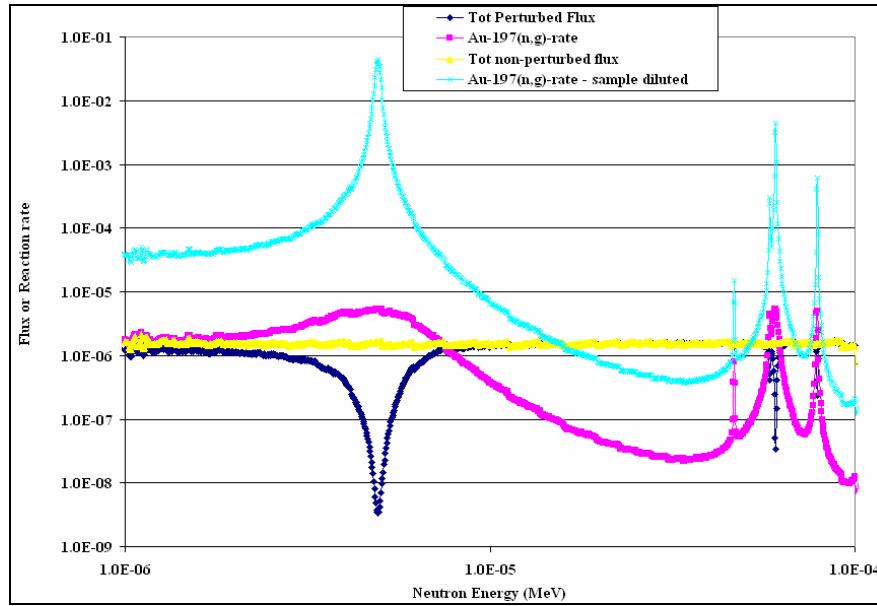


Graphic 3: Reaction rate versus the ratio “diluted density”/real density for a gold.

In graphic 4 the perturbed neutron fluxes and the reaction rate are depicted. The effect of self-shielding is clearly outlined for Au-197-diluted sample.



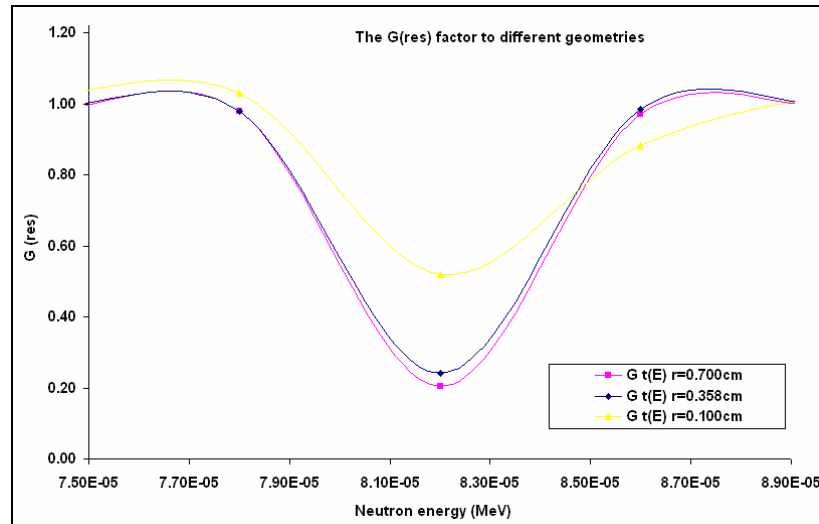
Graphic 4: neutron flux or reaction rate versus neutron energy (MeV) for gold.



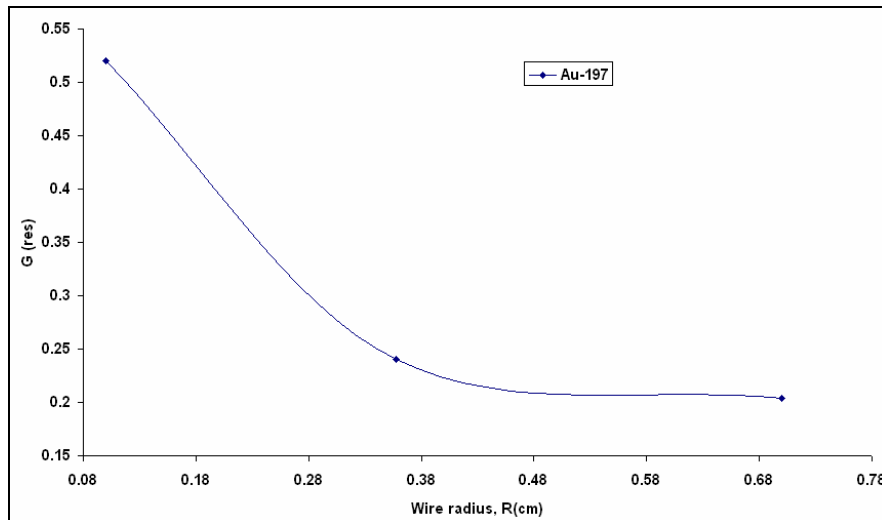
Graphic 5: neutron flux or reaction rate versus neutron energy (MeV) for gold.

Graphic 5 depicts the flux and reaction rate for Au-197 as a function of the incident neutron energies. The perturbed and non-perturbed fluxes and the corresponding reaction rates for diluted sample and “real” sample are exhibited. For the diluted sample the reaction rate exhibits a higher peak compared to reaction rate of “real” sample. The results are in good agreement with those by Gonçalves et al. [8].

Graphic 6 and 7 show the curve of $G_{(res)}$ factor of Au-197 as energy function for various wire radius. In the both cases the curves indicate a decrease of $G_{(res)}$ as the radius increases. The calculation were carried out using 1, 3.58 and 7mm radius wire..



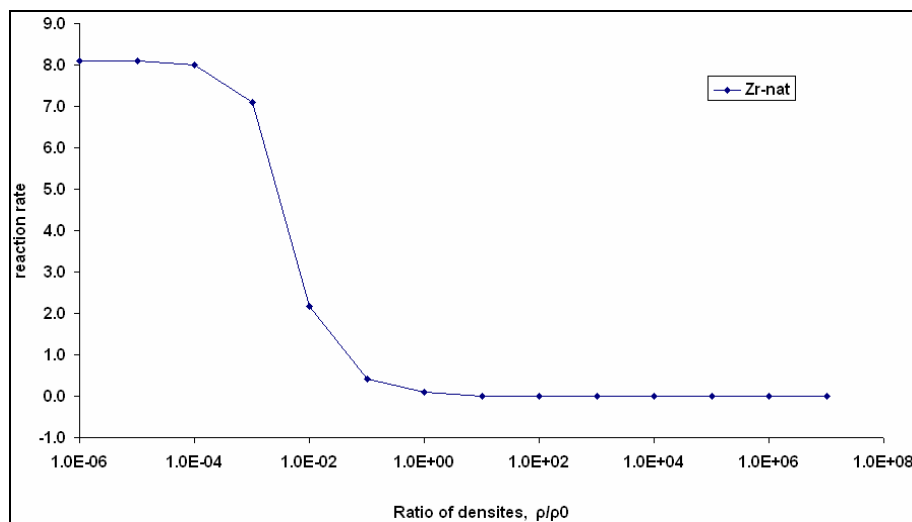
Graphic 6: Variation of the energy dependent resonance self-shielding factor of gold wire of different radii with neutron energy.



Graphic 7: Variation of resonance self-shielding factors of gold as function of the wire radius.

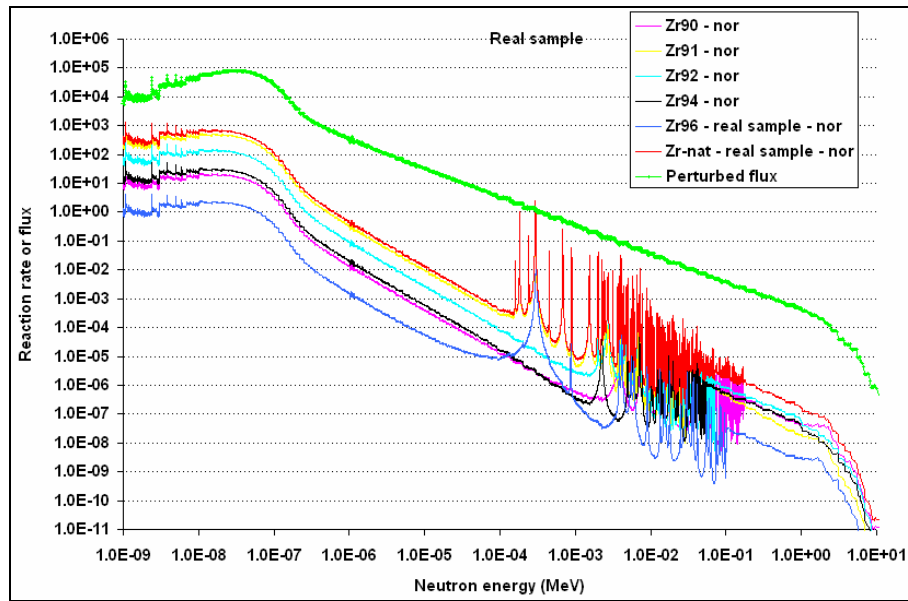
6.2. Zr foils and ZrO₂ powders

First of all it was necessary determine the saturation density of Zr before starting the calculations for the self-shielding factor. Numerical simulations considering different Zr material densities were done. The saturation curve obtained is displayed in graphic 8.

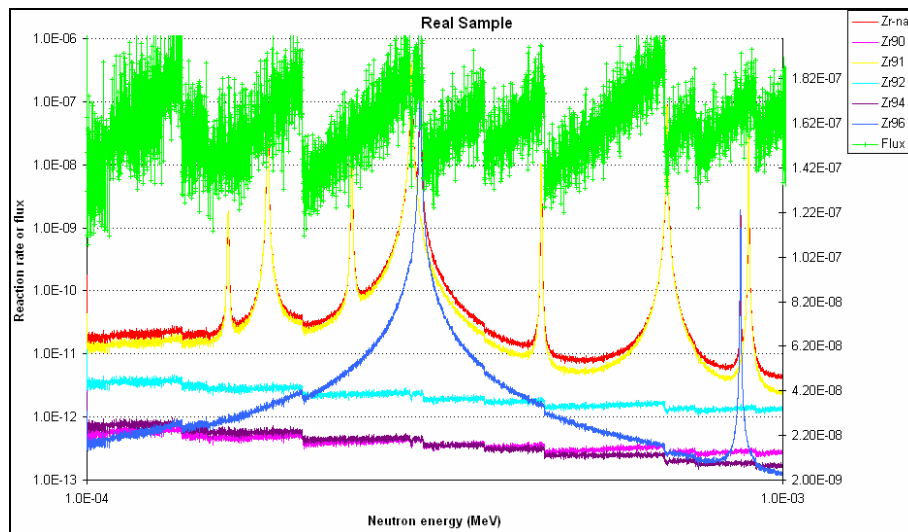


Graphic 8: Reaction rate versus the ratio "diluted density"/real density for a Zr foils.

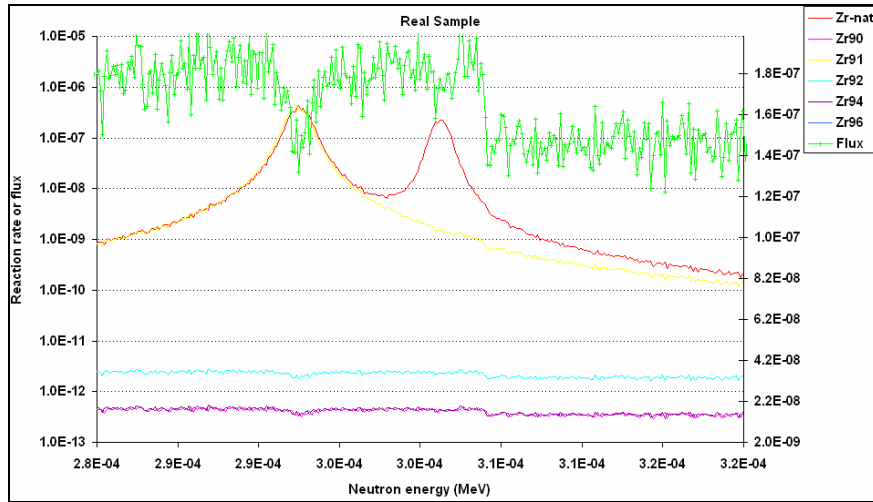
Graphic 9 shows the neutron spectrum (perturbed flux) and reaction rates of the various isotopes of the real Zr-foil sample. . These are Zr-90, Zr-91, Zr-92, Zr-94 and Zr-96. The later being of most interest in this work since the dosimeter is based on its activation is. In the graphic 10 the reaction rate and the flux are shown in the resonance energy range (from 100 eV to 1 keV).



Graphic9: Spectrum of reaction rate of real sample for each isotopic Zr and perturbed-flux

Graphic 10: Reaction rate spectrum of each isotopic Zr and perturbed-flux.
View in 1.0e-4 and 1.0e-3 MeV energies.

To calculate the Zr-96 self-shielding factor, G_{res} , we have considered its reaction rate in the energy window where cross-section exhibits resonance peaks. The corresponding neutron spectrum exhibits dips. For Zr-96 one has an isolated resonance in the energy span from 280eV and 320eV (see graphic 11).



Graphic 11: Spectrum of reaction rate of real sample of each isotopic Zr and perturbed-flux, view in 2.8e-4 and 3.2e-4 MeV of energies.

Taking the capture rate ratio between the actual sample and the diluted one, we could derive the G_{res} self-shielding factor. Using the same approach while considering the overall energy reaction rate, we calculated the effective self-shielding factor, G_{eff} .

The epithermal self-shielding factor G_{ep} and M_{ep} factor of Zr and ZrO₂ were calculated according to equation 9 and 10 respectively from Chilian et al. [5]. Table 4 shows the self-shielding factors G_{res} and G_{epi} of Zirconium sample.

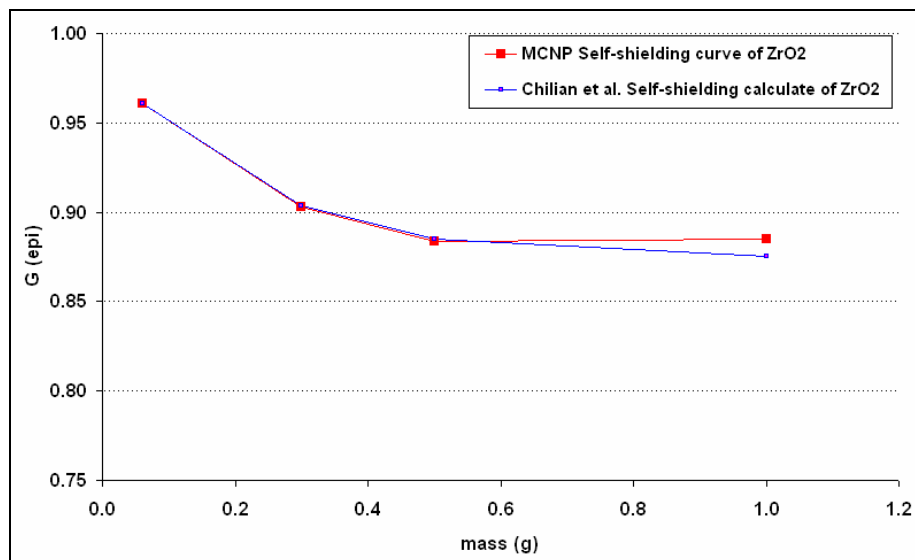
G(res) Self-shielding factor to Zr-96:		
G_{res}		0.95
G_{eff}		0.95

Table 4: G_{res} and G_{eff} factors of Zr calculate with MCNP code

For ZrO₂ powder samples the self-shielding factors of ⁹⁶Zr were calculated using 60 mg, 300 mg, 500 mg and 1000 mg sample masses. In table 5 the G_{ep} and M_{ep} factors obtained are collected. The agreement with values found in Chilian et al. [5] is excellent.

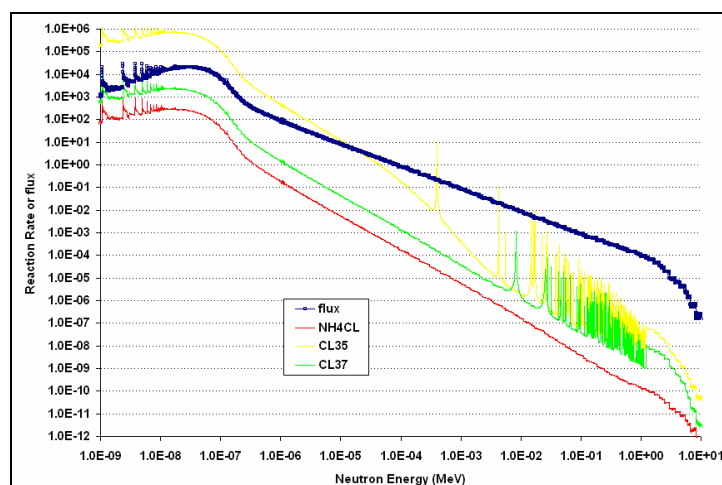
Description	M _{ep}	mass Zirconium	Chilian et al. G _{ep}	Present study G _{ep}
Zr foil 1	1.9E+03	0.02	0.97	-
Zr foil 5	2.2E+03	0.07	0.90	-
Zr foil 20	3.2E+03	0.22	0.79	-
ZrO ₂ 0,06	4.0E+03	0.06	0.96	0.960
ZrO ₂ 0,3	5.7E+03	0.3	0.90	0.903
ZrO ₂ 0,5	7.5E+03	0.5	0.88	0.884
ZrO ₂ 1	1.3E+04	1	0.88	0.885

Table 5: G_{ep} and M_{ep} factors of Zr and ZrO₂

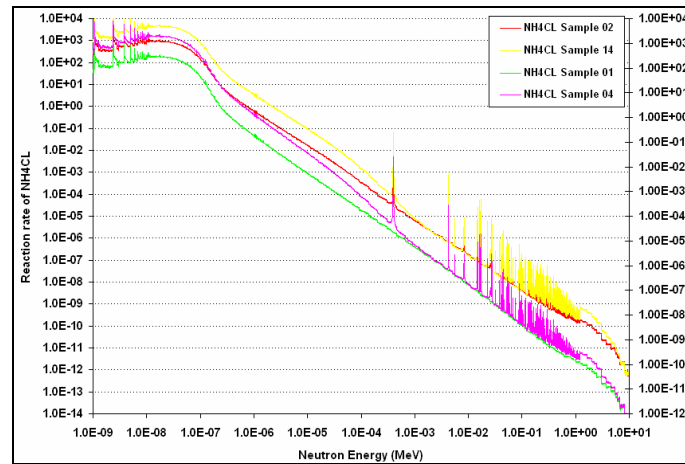
Graphic 12: Self-shielding factor as a function of the thickness of ZrO₂.

6.3. Chlorine sample

In graphic 13 the reaction rates calculated in non-perturbed flux are plotted. . This pure glucose sample is indeed considered as the non-perturbed case. . No local depression is observed in the neutron spectrum since there the concentration of Cl is zero. Graphic 14 show the similar curves for sample mixtures with increasing Cl concentrations. Now the the mixture reaction rate exhibits resonance features.

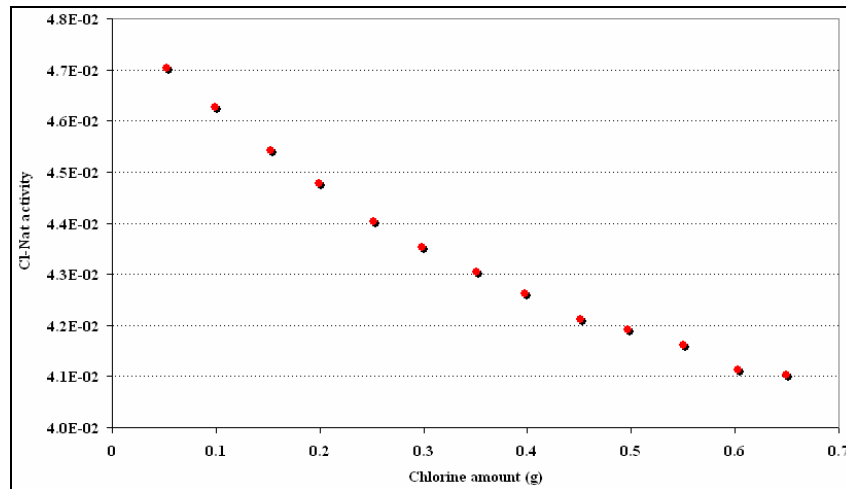


Graphic 13: the curve of chlorine, sample 01.



Graphic 14: the curve of NH4CL.

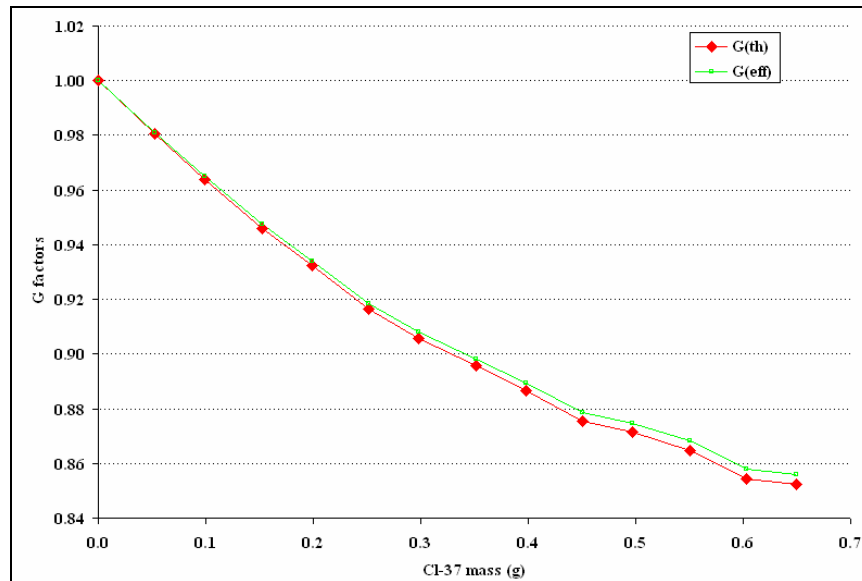
The graphic 15 is shows the activity rate of Cl-Nat calculated by MCNP as function the Cl amount in the sample.



Graphic 15: the curve of activity rate as function Chlorine-Nat amount (g)

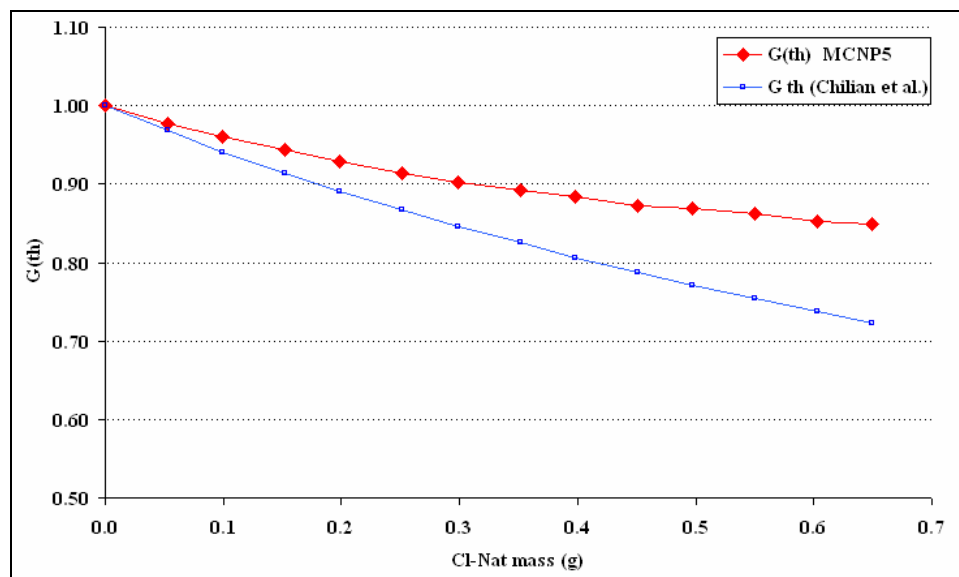
To calculate the Cl-37 self-shielding factor, G_{res} , we have considered its reaction rate in the energy window where cross-section exhibits resonance peaks. The corresponding neutron spectrum exhibits dips. For Cl-37 one has an isolated resonance in the energy-span from 389.5eV and 420.25eV. Taking the capture rate ratio between the “real” sample and the diluted one, we could derive the G_{res} self-shielding factor.

Using the same approach while considering the overall energy reaction rate, we calculated the effective self-shielding factor, G_{eff} . In addition the thermal self-shielding factor, G_{th} was calculated take into account the total energy span from 0eV and 0.55eV. The graphic 16 shows the shelf-shielding factors as function the amount of Cl in gram present in the sample.



Graphic 16: the curve of G factors as function Chlorine-37 amount (g).

Graphic 17 compares the thermal shelf-shielding factor, G_{th} , as function the Cl concentration calculated using equation of Chilian et al. [5] and to the values the G_{th} factors derived using reaction rates calculated by MCNP5. The values from Chilian et al. are lower and become lower and lower as the mass of ammonium chlorine increases. From the paper of Chilian, it is not specified the mixture matrix (here $C_6H_{12}O_6$) and the chlorine substance (here NH_4Cl). Due to the presence of hydrogen and carbon are very effective neutron scattering at moderating atoms. This may explain the increase of G_{th} in the $NH_4Cl-C_6H_{12}O_6$ mixture. In table 6 are gathered the results of G factors obtained from MCNP simulation for Chlorine sample.

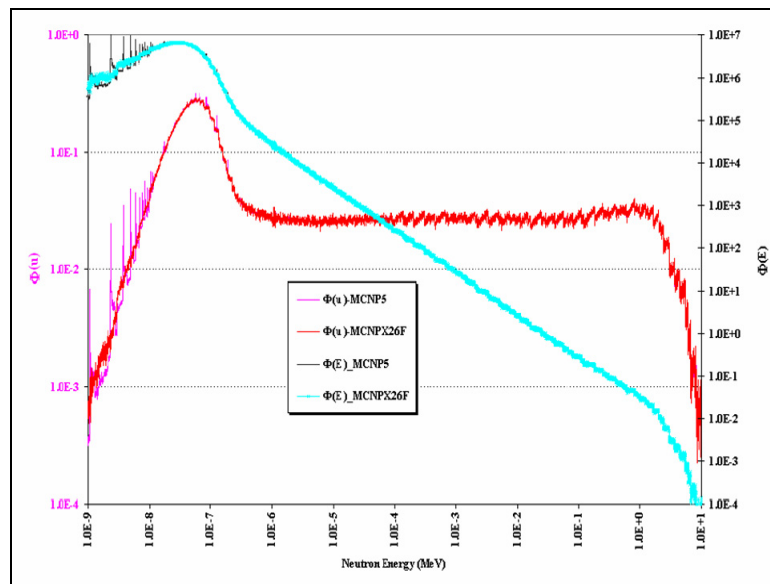


Graphic 17: the curve of Gth as function Chlorine-Nat amount (g) using the equation of Chilian et al. and result founded in MCNP5 case

Self-shielding factor of Chlorine:	Values:
G(res)	0.89
G(eff)	0.86
G(th)	0.85

Table 6: Gres and Geff factors of Cl calculate with MCNP code

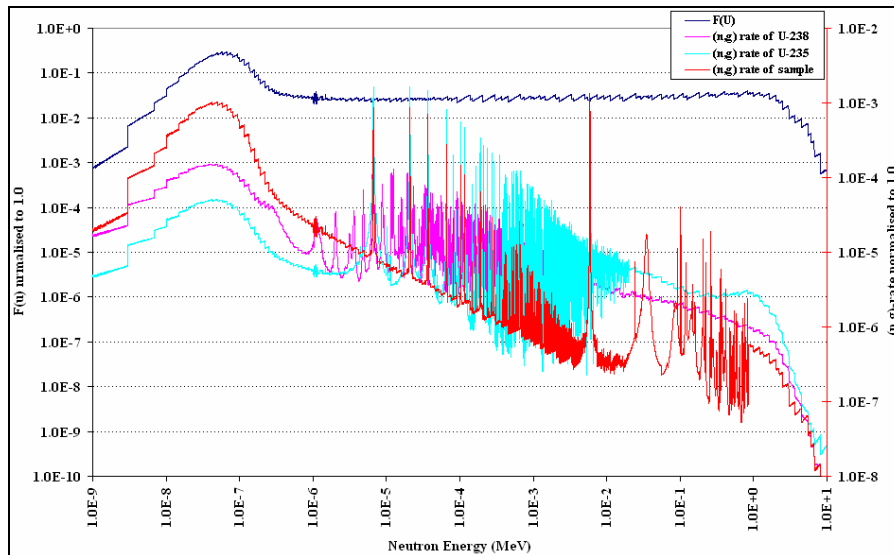
Graphic 18 shows the neutron spectrum obtained in the pure glucose $C_6H_{12}O_6$ (sugar) sample. The spectrum obtained using MCNP5 code exhibits tilts in the cold neutron energy region (below $E=kT$). Below the thermal region, there is no physical reason to have such features. Such unphysical tilts have been reported earlier and arise from an unsatisfactory treatment of $S(\alpha,\beta)$ scattering law by MCNP5. Running the same problem using the MCNPX 2.6.0, we got a spectrum free of this tilts (see Figure 18)



Graphic18: MCNP5 Vs MCNPX26F S(a,b) law used for $C_6H_{12}O_6$

6.4. Uranium samples

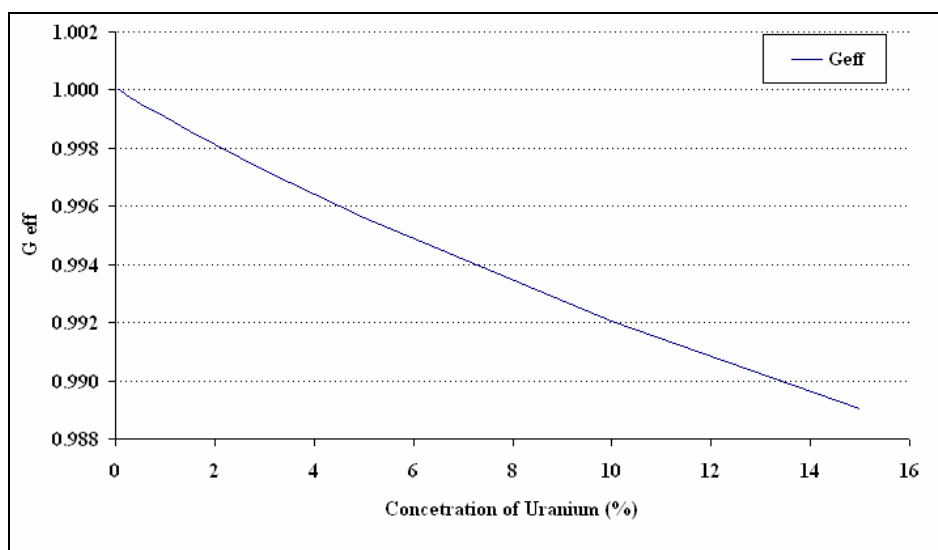
In graphics 19 is possible to see the perturbed neutron spectrum normalized to 1.0 together with the (n,γ) rate of sample, U-235 and U-235 as function energy in MeV. That result was obtained of wire sample.



Graphics 19: Flux and (n,γ) rate of wire sample

The G_{eff} -factors obtained for various samples containing U are collected in Table 7. Graphic 20 show G_{eff} of Uranium wire sample plotted as a function of the U concentration. As for the other samples studied thus far, the G_{eff} -factors decrease with the increase of U amount.

SAMPLE	KID	Description	G_{eff}
1	FOIL	Foil with Aluminium=99,8% and Uranium=0.2%	1.0334
2	WIRE	Wire with Aluminium=99,8% and Uranium=0.2%	0.9934
3	Powder	UO ₂ - Uranium=85,5% Oxide=14,5%	0.7956
4	FILTER 5.0	Filter spiked with Uranium diluted in water	0.9952
	FILTER (Cellulose)	Filter (Cellulose) + U+H ₂ O (100ppm Uranium)	
5	Liquid	LIQUID with U + H ₂ O (U diluted 100 ppm)	1.0496

Table 7: G_{res} and G_{eff} factors of Cl

Graphics 20: G factors to Uranium with different concentrations.

7. Conclusions

The self-shielding factors G_{th} , G_{epi} or G_{res} , and G_{eff} have been investigated for various sets of dosimeter samples including gold, zirconium, chlorine and uranium (wires and filters aqueous solution and oxide powder). The study was carried out by carrying out numerical simulations of the experimental set using MCNP5 and/or MCNPX.2.6.0 code versions along with nuclear data from JEFF3.1 library. The results obtained for more gold, zirconium and Chlorine agree perfectly with those obtained using the "universe" formulas established by Chilian et al. and Gonçalves et al. In the case of mixture containing chlorine the G_{th} factors calculated by this study are higher than those reported by Chilian about chlorine. This is likely due to the scattering and moderating of neutron by the hydrogen and carbon atoms in the glucose and ammonium matrix. Incoming fast and epithermal neutrons will be slowed down to thermal region increasing the absorption in the thermal region. For the same reason the G_{th} in U aqueous solutions or in cellulose filters are likely to exhibit the same trend.

8. References

1. MCNP — A General Monte Carlo N-Particle Transport Code, Version 5, “*Volume I: Overview and Theory*”, April 24, 2003 (Revised 6/30/04). Los Alamos National Laboratory Report LA-UR-03-1987.
2. MCNP — A General Monte Carlo N-Particle Transport Code, Version 5, “*Volume II: User’s Guide*”, April 24, 2003. Los Alamos National Laboratory Report LA-CP-03-0245.
3. MCNP — A General Monte Carlo N-Particle Transport Code, Version 5, “*Volume III: Developer’s Guide*”, April 24, 2003. Los Alamos National Laboratory Report LA-CP-03-0284
4. I. F. Gonçalves, E. Martinho, J. Salgado, in: Epithermal neutron self-shielding factors in foils for collimated beams. *Appl. Radiat. Isto.* 60 (2004) 677-681.
5. C. Chilian, J. St-Pierre, G. Kennedy, in: Dependence of thermal and epithermal neutron self-shielding on sample size and irradiation site. *Appl. Radiat. Isto.* 60 (2004) 677.
6. I. F. Gonçalves, E. Martinho, J. Salgado, in: Extension to cylindrical samples of the universal curve of resonance neutron self-shielding factors. *Nuclear Instruments and Methods in Physics Research B* 213 (2004) 186-188.
7. Tufic Madi Filho, Ruy Barros de Lima, Hélio Yoriyaz and Antonio Carlos Hernandez, in: Experimental and Monte Carlo evaluation of the neutron flux of an assembly with two AmBe sources. *Radiation Protection Dosimetry* (2005), Vol. 115, No 1-4, pp. 412-414.
8. I. F. Gonçalves, E. Martinho, J. Salgado, in: Monte Carlo calculation of epithermal neutron resonance self-shielding factors in wires of different materials. *Appl. Radiat. Isto.* 55 (2001) 447-451.
9. I. F. Gonçalves, E. Martinho, J. Salgado, in: Monte Carlo calculation of epithermal neutron resonance self-shielding factors in foils of different materials. *Appl. Radiat. Isto.* 56 (2002) 945-951.
10. Pierre Marie in: Neutron Self Shielding Factors Determination: Comparison between MCNP simulations , Kayzero tables and analytical formulas.
11. Annual Book of ASTM Standards: Nuclear, Sola, and Geothermal Energy. Vol. 12.02 - 1997
12. Pytel Krzysztof, Jozefowicz Krystyna, Pytel Beatrycze, Koziel Alina. Self-shielding effects in neutron spectra measurements for neutron capture therapy by means of activation foils. *Radiation protection dosimetry* ISSN 0144-8420 CODEN RPDODE, 2004, vol. 110, no1-4, pp. 823-826.
13. Parry. Susan J. Activation Spectrometry in Chemical Analysis (*Chemical Analysis: A Series of Monographs on Analytical Chemistry and Its Applications*). V 119. 1991.
14. Briesmeister JF. MCNP – A general monte carlo n-particle transport code, version 4C. Los Alamos: LA-13709-M; 2000.
15. E. Martinho, J. Salgado, I. F. Gonçalves in: Universal curve of the thermal neutron self-shielding factor in foils, wires, spheres and cylinders. *Journal of Radioanalytical and Nuclear Chemistry*, Vol 261. No.3 (2004)637-643.
16. Belgian Nuclear Research Centre – Research towards a sustainable option. Available in: <<http://www.sckcen.be/en/Our-Services/Reactor-and-nuclear-measurements/Neutron-activation-analysis>> Access in 01 of September of 2008.

17. National Nuclear Data Center - NNDC – Available in: <<http://www.nndc.bnl.gov/exfor/endl00.htm>> Access in 23 of September of 2008.
18. Data T2 Nuclear Information Service – Available in: < <http://t2.lanl.gov/data/>> Access in 01 of October of 2008.
19. J.K.Shultis, R.E. Faw - MCNP - An MCNP PRIMER, 2004-2006. Dept. of Mechanical and Nuclear Engineering / Kansas State University Manhattan, KS 66506.
20. BR1 - 50th anniversary –SCK.CEN – Available in: < <http://www.sckcen.be/BR1/> > access in 08 of November of 2008.
21. W. Haeck and B. Verboomen, ZZ ALEPH-LIB-JEFF3.1, MCNP Neutron Cross Section Library based on JEFF3.1; <http://www.nea.fr/abs/html/nea-1745.html>

Appendix A

Input file standard used to calculate the reaction rate of Au, Zr, ZrO₂ and Cl.

```

MESSAGE: xsdir=xsdir31

MCNP  Neutron Self Shielding Determination - Chlorine vial R (SUGAR+0.65g CL)
c
c =====
c           Cell cards
c =====
c
1  1 -0.00120 -1 30  imp:n=1  $ Sample region(air)
2  2 -0.95  1 -2    imp:N=1  $ Sample region(HDPE)
3  3  0  2 -4      imp:N=1  $ Void region
4  4  0  4 -20     imp:N=1  $ void sphere
100 0  20         imp:N=0   $ Outside world
5  5 3 -0.67205 -30 imp:N=1  $ sample SUGAR+0.65g CL

c =====
c           Surface cards
c =====
1  rcc  0.0 0.0 -0.744 0.0 0.0 1.40 0.495 $sample incylinder
2  rcc  0.0 0.0 -0.825 0.0 0.0 1.65 0.570 $sample outcylinder
4  So   5                      $sphere
20 So   6                      $void sphere
30 rcc  0.0 0.0 -0.744 0.0 0.0 1.32 0.495 $sample SUGAR+NH4CL

c =====
c           Materials
c =====
c Material #1
c Air 78% Nitrogenio + 22% Oxi.
m1  nlib=03c
7014 3.80595E-05
7015 1.41343E-07
8016 1.02645E-05
18036 7.74926E-10
18038 1.44868E-10
18040 2.29029E-07
6000 7.33878E-09

c -----
c Material #2
c Polyethylene
m2  nlib=03c
1001 2 6000 1
mt2 poly.60t

c -----
c Material #3: SUGAR+NH4CL
m3  nlib=03c
6000 -1.1250
1001 -7.7500
8016 -0.5000
7014 -25.5614
7015 -0.1016
17035 -48.5462
17037 -16.4081

mt3 poly.60t
c
c
m35 17035.03c 1
m37 17037.03c 1
c
c =====
c           Mode
c =====
mode N

c =====
c           Source
c =====
sdef sur=4 nrm=-1 erg=d2
si2 H
1.00E-11 3.00E-09 5.00E-09 6.90E-09 1.00E-08
1.50E-08 2.00E-08 2.50E-08 3.00E-08 3.50E-08
4.20E-08 5.00E-08 5.80E-08 6.70E-08 7.70E-08
8.00E-08 9.50E-08 1.00E-07 1.15E-07 1.34E-07
1.40E-07 1.60E-07 1.80E-07 1.89E-07 2.20E-07
2.48E-07 2.80E-07 3.00E-07 3.15E-07 3.20E-07
3.50E-07 3.91E-07 4.00E-07 4.33E-07 4.85E-07
5.00E-07 5.40E-07 6.25E-07 7.05E-07 7.80E-07
7.90E-07 8.50E-07 8.60E-07 9.10E-07 9.30E-07

```

```

9.50E-07 9.72E-07 9.86E-07 9.96E-07 1.02E-06
1.04E-06 1.05E-06 1.07E-06 1.10E-06 1.11E-06
1.13E-06 1.15E-06 1.17E-06 1.24E-06 1.30E-06
1.34E-06 1.37E-06 1.45E-06 1.48E-06 1.50E-06
1.59E-06 1.67E-06 1.76E-06 1.84E-06 1.93E-06
2.02E-06 2.10E-06 2.13E-06 2.36E-06 2.55E-06
2.60E-06 2.72E-06 2.77E-06 3.30E-06 3.38E-06
4.00E-06 4.13E-06 5.04E-06 5.35E-06 6.16E-06
7.52E-06 8.32E-06 9.19E-06 9.91E-06 1.12E-05
1.37E-05 1.59E-05 1.95E-05 2.26E-05 2.50E-05
2.76E-05 3.05E-05 3.37E-05 3.73E-05 4.02E-05
4.55E-05 4.83E-05 5.16E-05 5.56E-05 6.79E-05
7.57E-05 9.17E-05 1.37E-04 1.49E-04 2.04E-04
3.04E-04 3.72E-04 4.54E-04 6.77E-04 7.49E-04
9.14E-04 1.01E-03 1.23E-03 1.43E-03 1.51E-03
2.03E-03 2.25E-03 3.35E-03 3.53E-03 5.00E-03
5.53E-03 7.47E-03 9.12E-03 1.11E-02 1.50E-02
1.66E-02 2.48E-02 2.74E-02 2.93E-02 3.70E-02
4.09E-02 5.52E-02 6.74E-02 8.23E-02 1.11E-01
1.23E-01 1.83E-01 2.47E-01 2.73E-01 3.02E-01
4.08E-01 4.50E-01 4.98E-01 5.50E-01 6.08E-01
8.21E-01 9.07E-01 1.00E+00 1.11E+00 1.22E+00
1.35E+00 1.65E+00 2.02E+00 2.23E+00 2.47E+00
3.01E+00 3.68E+00 4.49E+00 5.49E+00 6.07E+00
6.70E+00 8.19E+00 1.00E+01 1.16E+01 1.38E+01
1.49E+01 1.73E+01 1.96E+01
sp2 D
0.00E+00 1.17E+00 2.27E+00 2.11E+00 5.00E+00
1.15E+01 1.37E+01 1.53E+01 1.61E+01 1.57E+01
2.20E+01 2.33E+01 2.11E+01 2.08E+01 1.93E+01
5.12E+00 2.17E+01 5.85E+00 1.40E+01 1.26E+01
2.96E+00 7.69E+00 5.25E+00 1.82E+00 4.91E+00
3.09E+00 2.66E+00 1.44E+00 9.19E-01 3.32E-01
1.69E+00 1.96E+00 3.77E-01 1.36E+00 1.89E+00
5.06E-01 1.23E+00 2.28E+00 1.86E+00 1.52E+00
1.89E-01 1.07E+00 1.82E-01 8.15E-01 3.22E-01
3.15E-01 3.15E-01 2.21E-01 1.49E-01 3.36E-01
2.05E-01 1.32E-01 3.47E-01 3.44E-01 1.78E-01
1.95E-01 3.03E-01 2.52E-01 7.67E-01 7.22E-01
4.06E-01 3.42E-01 7.54E-01 2.76E-01 2.28E-01
8.15E-01 6.64E-01 6.84E-01 6.58E-01 6.51E-01
6.24E-01 5.24E-01 1.88E-01 1.38E+00 1.04E+00
2.73E-01 6.13E-01 2.42E-01 2.33E+00 3.19E-01
2.29E+00 4.45E-01 2.67E+00 7.62E-01 1.86E+00
2.61E+00 1.30E+00 1.35E+00 1.01E+00 1.66E+00
2.66E+00 2.00E+00 2.70E+00 1.99E+00 1.36E+00
1.36E+00 1.38E+00 1.35E+00 1.37E+00 1.02E+00
1.75E+00 8.05E-01 9.28E-01 1.03E+00 2.80E+00
1.50E+00 2.66E+00 5.62E+00 1.15E+00 4.49E+00
5.66E+00 2.82E+00 2.86E+00 5.76E+00 1.43E+00
2.88E+00 1.44E+00 2.90E+00 2.18E+00 7.18E-01
4.36E+00 1.46E+00 5.81E+00 7.20E-01 5.09E+00
1.46E+00 4.42E+00 2.96E+00 2.97E+00 4.41E+00
1.48E+00 5.97E+00 1.49E+00 1.02E+00 3.52E+00
1.55E+00 4.61E+00 3.02E+00 3.11E+00 4.71E+00
1.58E+00 6.40E+00 5.04E+00 1.65E+00 1.68E+00
5.18E+00 1.74E+00 1.78E+00 1.79E+00 1.78E+00
5.33E+00 1.81E+00 1.80E+00 1.76E+00 1.75E+00
1.71E+00 3.38E+00 3.06E+00 1.26E+00 1.19E+00
1.76E+00 1.09E+00 8.94E-01 7.10E-01 2.23E-01
1.51E-01 1.54E-01 6.64E-02 1.37E-02 5.68E-03
5.86E-04 4.10E-04 0.00E+00
c
=====
c
Tallies
c
=====
fc4 Average flux in the sample cell
f4:n 5
fm4 (1.0) ( -1 3 102)
(0.7577 35 102)
(0.2423 37 102)
e4 0.55e-6 0.1 1.0 20
fq4 f m e
c
fc104 Average flux in the sample cell $ of number reaction per cm3 of type 102 (n,y) in cell 5
f104:n 5
fm104 (1.0) ( -1 3 102)
(0.7577 35 102)
(0.2423 37 102)
fq104 f e m
e104 1.0000E-10
1.0000E-09 1.0046E-09 1.0093E-09 1.0139E-09 1.0186E-09 1.0233E-09
1.0280E-09 1.0328E-09 1.0375E-09 1.0423E-09 1.0471E-09 1.0520E-09
1.0568E-09 1.0617E-09 1.0666E-09 1.0715E-09 1.0765E-09 1.0814E-09
1.0864E-09 1.0914E-09 1.0965E-09 1.1015E-09 1.1066E-09 1.1117E-09
.....

```

```

1.0000E+00 1.0233E+00 1.0471E+00 1.0715E+00 1.0965E+00 1.1220E+00
1.1482E+00 1.1749E+00 1.2023E+00 1.2303E+00 1.2589E+00 1.2882E+00
1.3183E+00 1.3490E+00 1.3804E+00 1.4125E+00 1.4454E+00 1.4791E+00
1.5136E+00 1.5488E+00 1.5849E+00 1.6218E+00 1.6596E+00 1.6982E+00
1.7378E+00 1.7783E+00 1.8197E+00 1.8621E+00 1.9055E+00 1.9498E+00
1.9953E+00 2.0417E+00 2.0893E+00 2.1380E+00 2.1878E+00 2.2387E+00
2.2909E+00 2.3442E+00 2.3988E+00 2.4547E+00 2.5119E+00 2.5704E+00
2.6303E+00 2.6915E+00 2.7542E+00 2.8184E+00 2.8840E+00 2.9512E+00
3.0200E+00 3.0903E+00 3.1623E+00 3.2359E+00 3.3113E+00 3.3884E+00
3.4674E+00 3.5481E+00 3.6308E+00 3.7154E+00 3.8019E+00 3.8905E+00
3.9811E+00 4.0738E+00 4.1687E+00 4.2658E+00 4.3652E+00 4.4668E+00
4.5709E+00 4.6774E+00 4.7863E+00 4.8978E+00 5.0119E+00 5.1286E+00
5.2481E+00 5.3703E+00 5.4954E+00 5.6234E+00 5.7544E+00 5.8884E+00
6.0256E+00 6.1660E+00 6.3096E+00 6.4566E+00 6.6069E+00 6.7608E+00
6.9183E+00 7.0795E+00 7.2444E+00 7.4131E+00 7.5858E+00 7.7625E+00
7.9433E+00 8.1283E+00 8.3177E+00 8.5114E+00 8.7097E+00 8.9125E+00
9.1201E+00 9.3326E+00 9.5499E+00 9.7724E+00 1.0000E+01 2.0000E+01
c
c =====
nps      25000000000
prdmpr  0 5000000000 0 1 0
print
c =====

```

Appendix B

Output file standard used to analysis the results of MCNP.

```

Thread Name & Version = MCNP5_RSICC, 1.40

+-----+
| This program was prepared by the Regents of the University of |
| California at Los Alamos National Laboratory (the University) under |
| contract number W-7405-ENG-36 with the U.S. Department of Energy |
| (DoE). The University has certain rights in the program pursuant to |
| the contract and the program should not be copied or distributed |
| outside your organization. All rights in the program are reserved |
| by the DoE and the University. Neither the U.S. Government nor the |
| University makes any warranty, express or implied, or assumes any |
| liability or responsibility for the use of this software. |
+-----+

lmcnp version 5.mpi ld=02082007 11/09/08 20:03:22
*****
i=samp04 n=samp04.

1- MESSAGE: xsdir=xsdir31
2-
3- MCNP Neutron Self Shielding Determination - Chlorine vial R (SUGAR)
4- c
5- c ++++++
6- c running command: "/mcnp_pstudy.pl -i gluglu -setup -verbose ++++++
7- c ++++++
8- c
9- c
10- c
11- c
12- c =====
13- c Cell cards
14- c =====
15- c
16- 1 1 -0.00120 -1 3 imp:n=1 $ Sample region(air)
17- 2 2 -0.95 -2 1 imp:n=1 $ Sample region(HDPE)
18- 3 1 -0.00120 -4 2 imp:n=1 $ Void region
19- 4 0 -20 4 imp:n=1 $ void sphere
20- 5 3 -0.95330 -1 -3 imp:n=1 $ Sample powder(air)
21- 100 0 20 imp:n=0 $ Outside world
22-
23- c =====
24- c Surface cards
25- c =====
26- 1 rcc 0.0 0.0 -0.744 0.0 0.0 1.49 0.495 $$sample SUGAR
27- 2 rcc 0.0 0.0 -0.825 0.0 0.0 1.65 0.570 $$sample outcylinder
28- 3 pz 0.575
29- 4 So 10 $sphere
30- 20 So 11 $void sphere
31-
32- c =====
33- c Materials

```

```

34- c =====
35- c Material #1
36- c Air 78% Nitrogenio + 22% Oxi.
37- m1 nlib=03c
38- 6000 7.33878E-09
39- 7014 3.82008E-05
40- 8016 1.02645E-05
41- 18036 7.74926E-10 18038 1.44868E-10 18040 2.29029E-07
42- c -----
43- c Material #2
44- c Polyethylene
45- m2 nlib=03c
46- 1001 2
47- 6000 1
48- mt2 poly.60t
49- c -----
50- c Material #3: SUGAR (C6H12O6 + NH4Cl) mixture
51- m3 nlib=03c
52- 1001 -0.069032808
53- 6000 -0.3080616
54- 8016 -0.4102406
55- 7014 -0.06021469
56- 17035 -0.1139351
57- 17037 -0.03851534
58- mt3 poly.60t
59- c
60- m35 17035.03c 1
warning. material 35 is used only for a perturbation or tally.
61- m37 17037.03c 1
warning. material 37 is used only for a perturbation or tally.
62- c
63- c
64- c =====
65- c Mode
66- c =====
67- mode N
68- c =====
69- c Source
70- c =====
71- sdef sur=4 nrm=-1 erg=d2
72- si2 H
73- 1.00E-11 3.00E-09 5.00E-09 6.90E-09 1.00E-08
74- 1.50E-08 2.00E-08 2.50E-08 3.00E-08 3.50E-08
75- 4.20E-08 5.00E-08 5.80E-08 6.70E-08 7.70E-08
76- 8.00E-08 9.50E-08 1.00E-07 1.15E-07 1.34E-07
77- 1.40E-07 1.60E-07 1.80E-07 1.89E-07 2.20E-07
78- 2.48E-07 2.80E-07 3.00E-07 3.15E-07 3.20E-07
79- 3.50E-07 3.91E-07 4.00E-07 4.33E-07 4.85E-07
80- 5.00E-07 5.40E-07 6.25E-07 7.05E-07 7.80E-07
81- 7.90E-07 8.50E-07 8.60E-07 9.10E-07 9.30E-07
82- 9.50E-07 9.72E-07 9.86E-07 9.96E-07 1.02E-06
83- 1.04E-06 1.05E-06 1.07E-06 1.10E-06 1.11E-06
84- 1.13E-06 1.15E-06 1.17E-06 1.24E-06 1.30E-06
85- 1.34E-06 1.37E-06 1.45E-06 1.48E-06 1.50E-06
86- 1.59E-06 1.67E-06 1.76E-06 1.84E-06 1.93E-06
87- 2.02E-06 2.10E-06 2.13E-06 2.36E-06 2.55E-06
88- 2.60E-06 2.72E-06 2.77E-06 3.30E-06 3.38E-06
89- 4.00E-06 4.13E-06 5.04E-06 5.35E-06 6.16E-06
90- 7.52E-06 8.32E-06 9.19E-06 9.91E-06 1.12E-05
91- 1.37E-05 1.59E-05 1.95E-05 2.26E-05 2.50E-05
92- 2.76E-05 3.05E-05 3.37E-05 3.73E-05 4.02E-05
93- 4.55E-05 4.83E-05 5.16E-05 5.56E-05 6.79E-05
94- 7.57E-05 9.17E-05 1.37E-04 1.49E-04 2.04E-04
95- 3.04E-04 3.72E-04 4.54E-04 6.77E-04 7.49E-04
96- 9.14E-04 1.01E-03 1.23E-03 1.43E-03 1.51E-03
97- 2.03E-03 2.25E-03 3.35E-03 3.53E-03 5.00E-03
98- 5.53E-03 7.47E-03 9.12E-03 1.11E-02 1.50E-02
99- 1.66E-02 2.48E-02 2.74E-02 2.93E-02 3.70E-02
100- 4.09E-02 5.52E-02 6.74E-02 8.23E-02 1.11E-01
101- 1.23E-01 1.83E-01 2.47E-01 2.73E-01 3.02E-01
102- 4.08E-01 4.50E-01 4.98E-01 5.50E-01 6.08E-01
103- 8.21E-01 9.07E-01 1.00E+00 1.11E+00 1.22E+00
104- 1.35E+00 1.65E+00 2.02E+00 2.23E+00 2.47E+00
105- 3.01E+00 3.68E+00 4.49E+00 5.49E+00 6.07E+00
106- 6.70E+00 8.19E+00 1.00E+01 1.16E+01 1.38E+01
107- 1.49E+01 1.73E+01 1.96E+01
108- sp2 D
109- 0.00E+00 1.17E+00 2.27E+00 2.11E+00 5.00E+00
110- 1.15E+01 1.37E+01 1.53E+01 1.61E+01 1.57E+01
111- 2.20E+01 2.33E+01 2.11E+01 2.08E+01 1.93E+01
112- 5.12E+00 2.17E+01 5.85E+00 1.40E+01 1.26E+01
113- 2.96E+00 7.69E+00 5.25E+00 1.82E+00 4.91E+00
114- 3.09E+00 2.66E+00 1.44E+00 9.19E-01 3.32E-01
115- 1.69E+00 1.96E+00 3.77E-01 1.36E+00 1.89E+00
116- 5.06E-01 1.23E+00 2.28E+00 1.86E+00 1.52E+00
117- 1.89E-01 1.07E+00 1.82E-01 8.15E-01 3.22E-01

```

```

118-      3.15E-01 3.15E-01 2.21E-01 1.49E-01 3.36E-01
119-      2.05E-01 1.32E-01 3.47E-01 3.44E-01 1.78E-01
120-      1.95E-01 3.03E-01 2.52E-01 7.67E-01 7.22E-01
121-      4.06E-01 3.42E-01 7.54E-01 2.76E-01 2.28E-01
122-      8.15E-01 6.64E-01 6.84E-01 6.58E-01 6.51E-01
123-      6.24E-01 5.24E-01 1.88E-01 1.38E+00 1.04E+00
124-      2.73E-01 6.13E-01 2.42E-01 2.33E+00 3.19E-01
125-      2.29E+00 4.45E-01 2.67E+00 7.62E-01 1.86E+00
126-      2.61E+00 1.30E+00 1.35E+00 1.01E+00 1.66E+00
127-      2.66E+00 2.00E+00 2.70E+00 1.99E+00 1.36E+00
128-      1.36E+00 1.38E+00 1.35E+00 1.37E+00 1.02E+00
129-      1.75E+00 8.05E-01 9.28E-01 1.03E+00 2.80E+00
130-      1.50E+00 2.66E+00 5.62E+00 1.15E+00 4.49E+00
131-      5.66E+00 2.82E+00 2.86E+00 5.76E+00 1.43E+00
132-      2.88E+00 1.44E+00 2.90E+00 2.18E+00 7.18E-01
133-      4.36E+00 1.46E+00 5.81E+00 7.20E-01 5.09E+00
134-      1.46E+00 4.42E+00 2.96E+00 2.97E+00 4.41E+00
135-      1.48E+00 5.97E+00 1.49E+00 1.02E+00 3.52E+00
136-      1.55E+00 4.61E+00 3.02E+00 3.11E+00 4.71E+00
137-      1.58E+00 6.40E+00 5.04E+00 1.65E+00 1.68E+00
138-      5.18E+00 1.74E+00 1.78E+00 1.79E+00 1.78E+00
139-      5.33E+00 1.81E+00 1.80E+00 1.76E+00 1.75E+00
140-      1.71E+00 3.38E+00 3.06E+00 1.26E+00 1.19E+00
141-      1.76E+00 1.09E+00 8.94E-01 7.10E-01 2.23E-01
142-      1.51E-01 1.54E-01 6.64E-02 1.37E-02 5.68E-03
143-      5.86E-04 4.10E-04 0.00E+00
144-      c -----
145-      c =====
146-      c           Tallies
147-      c =====
148-      fc4  Average flux in the sample cell
149-      f4:n 5
150-      fm4  (1.0) (-1 3 102)(0.7577 35 102)(0.2423 37 102)
151-      e4   0.55e-6 0.1 1.0 20
152-      fq4  f m e
153-      c
154-      c
155-      fc14 flux and reaction rates within the sample
156-      f14:n 5
157-      fm14 (1.0) (-1 3 102)(0.7577 35 102)(0.2423 37 102)
158-      fq14 f e m
159-      e14  1.0000E-11 1.0046E-11 1.0093E-11 1.0139E-11 1.0186E-11 1.0233E-11
.....
1909-      1.0000E+01 2.0000E+01
1910-      c
1911-      c =====
1912-      nps  15000000000
1913-      prdmp 0 500000000 0 1 0
1914-      rand seed=207327
1915-      print
1916-      c =====
lsources                                print table 10

lmaterial composition                    print table 40

the sum of the fractions of material 1 was 4.870259E-05

the sum of the fractions of material 2 was 3.000000E+00

material
number  component nuclide, atom fraction

1      6000, 1.50686E-04  7014, 7.84369E-01  8016, 2.10759E-01  18036, 1.59114E-05
      18038, 2.97454E-06  18040, 4.70260E-03
2      1001, 6.66667E-01  6000, 3.33333E-01
associated thermal s(a,b) data sets: poly.60t
3      1001, 5.33492E-01  6000, 1.99763E-01  8016, 1.99762E-01  7014, 3.34916E-02
      17035, 2.53766E-02  17037, 8.11502E-03
associated thermal s(a,b) data sets: poly.60t
35     17035, 1.00000E+00
37     17037, 1.00000E+00

material
number  component nuclide, mass fraction

1      6000, 1.24433E-04  7014, 7.55141E-01  8016, 2.31767E-01  18036, 3.93462E-05
      18038, 7.76358E-06  18040, 1.29203E-02
2      1001, 1.43701E-01  6000, 8.56299E-01
3      1001, 6.90328E-02  6000, 3.08062E-01  8016, 4.10241E-01  7014, 6.02147E-02
      17035, 1.13935E-01  17037, 3.85153E-02
35     17035, 1.00000E+00

```



```

17037,1.00000E+00
warning. 2 materials had unnormalized fractions. print table 40.
1cell volumes and masses                                print table 50

  cell  atom    gram    input    calculated    reason volume
      density density volume  volume      mass      pieces not calculated

1  1  4.96832E-05  1.20000E-03  0.00000E+00  1.31630E-01  1.57957E-04  1
2  2  1.22358E-01  9.50000E-01  0.00000E+00  5.37205E-01  5.10345E-01  1
3  3  4.96832E-05  1.20000E-03  0.00000E+00  4.18711E+03  5.02453E+00  1
4  4  0.00000E+00  0.00000E+00  0.00000E+00  1.38649E+03  0.00000E+00  1
5  5  7.37083E-02  9.53300E-01  0.00000E+00  1.01532E+00  9.67909E-01  1
6  100 0.00000E+00  0.00000E+00  0.00000E+00  0.00000E+00  0.00000E+00  0  infinite

1surface areas                                print table 50

  surface  input    calculated    reason area
      area      area      not calculated

2  1.1  0.00000E+00  4.63416E+00
3  1.2  0.00000E+00  7.69769E-01
4  1.3  0.00000E+00  7.69769E-01
6  2.1  0.00000E+00  5.90934E+00
7  2.2  0.00000E+00  1.02070E+00
8  2.3  0.00000E+00  1.02070E+00
9  3  0.00000E+00  7.69769E-01
10 4  0.00000E+00  1.25664E+03
11 20 0.00000E+00  1.52053E+03

1cells                                print table 60

  cell  atom    gram    neutron
      mat density density volume  mass  pieces importance

1  1  1  4.96832E-05  1.20000E-03  1.31630E-01  1.57957E-04  1  1.0000E+00
2  2  2s 1.22358E-01  9.50000E-01  5.37205E-01  5.10345E-01  1  1.0000E+00
3  3  1  4.96832E-05  1.20000E-03  4.18711E+03  5.02453E+00  1  1.0000E+00
4  4  0  0.00000E+00  0.00000E+00  1.38649E+03  0.00000E+00  1  1.0000E+00
5  5  3s 7.37083E-02  9.53300E-01  1.01532E+00  9.67909E-01  1  1.0000E+00
6  100 0  0.00000E+00  0.00000E+00  0.00000E+00  0.00000E+00  0  0.0000E+00

total                                5.57528E+03  6.50294E+00
1surfaces                                print table 70

  surface  trans type  surface coefficients

1  1      rcc
2  1.1     cz  4.9500000E-01
3  1.2     pz  7.4600000E-01
4  1.3     p  0.0000000E+00  0.0000000E+00 -1.0000000E+00  7.4400000E-01
5  2      rcc
6  2.1     cz  5.7000000E-01
7  2.2     pz  8.2500000E-01
8  2.3     p  0.0000000E+00  0.0000000E+00 -1.0000000E+00  8.2500000E-01
9  3      pz  5.7500000E-01
10 4      so  1.0000000E+01
11 20     so  1.1000000E+01

1 cell temperatures in mev for the free-gas thermal neutron treatment.                                print table 72

all non-zero importance cells with materials have a temperature for thermal neutrons of 2.5300E-08 mev.

minimum source weight = 1.0000E+00  maximum source weight = 1.0000E+00

*****
* Random Number Generator = 1 *
* Random Number Seed = 207327 *
* Random Number Multiplier = 19073486328125 *
* Random Number Adder = 0 *
* Random Number Bits Used = 48 *
* Random Number Stride = 152917 *
*****

18036.03c 12262 180360 JEFF 3.1 library at 300 K - NJOY 99.112                                mat1825 12/05/05
          temperature = 2.5850E-08 adjusted to 2.5300E-08

          tables from file 180380_31.03c

18038.03c 13486 180380 JEFF 3.1 library at 300 K - NJOY 99.112                                mat1831 12/05/05
          probability tables used from 3.0000E-01 to 1.0000E+00 mev.
          temperature = 2.5850E-08 adjusted to 2.5300E-08

          tables from file 180400_31.03c

18040.03c 134682 180400 JEFF 3.1 library at 300 K - NJOY 99.112                                mat1837 12/05/05
          temperature = 2.5850E-08 adjusted to 2.5300E-08

          tables from file sab2002

```

poly.60t 69775 1-h-1 in polyethylene at 293.6k from endf-vi.5 njoy99.0 1001 0 0 09/14/99

total 794402

comment. 9 cross sections modified by free gas thermal treatment.
lassignment of s(a,b) data to nuclides.

print table 102

mat	nuclide	s(a,b)
2	1001.03c	poly.60t
3	1001.03c	poly.60t

dump no. 1 on file samp04.r nps = 0 coll = 0 ctm = 0.00 nrm = 0

3 warning messages so far.

1 starting mcrun. cp0 = 0.02 print table 110

MCNP Neutron Self Shielding Determination - Chlorine vial R (SUGAR)

master starting 19 tasks with 1 threads each 11/09/08 20:03:25

master set rendezvous nps = 200 11/09/08 20:03:25

FIRST RESULTS : TALLY 1

1tally 4 nps = 15000000000

+ Average flux in the sample cell
tally type 4 track length estimate of particle flux.
tally for neutrons
multiplier bin 1: 1.00000E+00
multiplier bin 2: -1.00000E+00 3 102
multiplier bin 3: 7.57700E-01 35 102
multiplier bin 4: 2.42300E-01 37 102

volumes
cell: 5
1.01532E+00

cell 5

energy:	5.5000E-07	1.0000E-01	1.0000E+00	2.0000E+01	total
mult bin					
1	1.74210E-03 0.0002	1.03057E-03 0.0002	2.23034E-04 0.0005	1.10500E-04 0.0007	3.10621E-03 0.0002
2	1.27121E-04 0.0002	3.23616E-06 0.0005	1.11161E-09 0.0014	3.72232E-10 0.0007	1.30359E-04 0.0002
3	4.41676E-02 0.0002	1.10902E-03 0.0005	2.16140E-07 0.0027	6.82745E-08 0.0008	4.52769E-02 0.0002
4	1.40257E-04 0.0002	4.02632E-06 0.0004	3.43325E-08 0.0028	1.07774E-08 0.0008	1.44328E-04 0.0002

SECOND RESULTS : TALLY 2

1tally 14 nps = 15000000000

+ flux and reaction rates within the sample
tally type 4 track length estimate of particle flux.
tally for neutrons
multiplier bin 1: 1.00000E+00
multiplier bin 2: -1.00000E+00 3 102
multiplier bin 3: 7.57700E-01 35 102
multiplier bin 4: 2.42300E-01 37 102

volumes
cell: 5
1.01532E+00

cell 5

mult bin:	1	2	3	4
energy				
1.0000E-11	9.51452E-12 0.5764	4.56041E-11 0.5764	1.58462E-08 0.5764	5.02916E-11 0.5764
1.0046E-11	0.00000E+00 0.0000	0.00000E+00 0.0000	0.00000E+00 0.0000	0.00000E+00 0.0000
1.0093E-11	0.00000E+00 0.0000	0.00000E+00 0.0000	0.00000E+00 0.0000	0.00000E+00 0.0000
1.0139E-11	0.00000E+00 0.0000	0.00000E+00 0.0000	0.00000E+00 0.0000	0.00000E+00 0.0000
1.0000E+01	4.56614E-09 0.1133	1.52279E-14 0.1133	1.15860E-12 0.1133	6.83608E-14 0.1133
2.0000E+01	1.21178E-07 0.0220	3.93798E-13 0.0222	3.56474E-11 0.0222	3.15749E-12 0.0322
total	3.10621E-03 0.0002	1.30359E-04 0.0002	4.52769E-02 0.0002	1.44328E-04 0.0002

8 warning messages so far.

run terminated when 15000000000 particle histories were done.

computer time = 2531.73 minutes

mcnp version 5.mpi 02082007

11/09/08 22:10:22

probid = 11/09/08 20:03:22